Development of Transition Metal Macrocyclic-Catalysts Supported on Multi-Walled Carbon Nanotubes for Alkaline Membrane Fuel Cell

by

QuratulAin Jawed Shah

A Thesis Presented in Partial Fulfillment
of the Requirements for the Degree
Master of Science in Technology

Approved April 2012 by the
Graduate Supervisory Committee:

Arunachalanadar Madakannan, Chair
Govindasamy Tamizhmani
Narciso Macia

ARIZONA STATE UNIVERSITY

May 2012

ABSTRACT

Low temperature fuel cells are very attractive energy conversion technology for automotive applications due to their qualities of being clean, quiet, efficient and good peak power densities. However, due to high cost and limited durability and reliability, commercialization of this technology has not been possible as yet. The high fuel cell cost is mostly due to the expensive noble catalyst Pt. Alkaline fuel cell (AFC) systems, have potential to make use of non-noble catalysts and thus, provides with a solution of overall lower cost. Therefore, this issue has been addressed in this thesis work.

Hydrogen-oxygen fuel cells using an alkaline anion exchange membrane were prepared and evaluated. Various non-platinum catalyst materials were investigated by fabricating membrane-electrode assemblies (MEAs) using Tokuyama membrane (# A201) and compared with commercial noble metal catalysts. Co and Fe phthalocyanine catalyst materials were synthesized using multi-walled carbon nanotubes (MWCNTs) as support materials. X-ray photoelectron spectroscopic study was conducted in order to examine the surface composition. The electroreduction of oxygen has been investigated on Fe phthalocyanine/MWCNT, Co phthalocyanine/MWCNT and commercial Pt/C catalysts. The oxygen reduction reaction kinetics on these catalyst materials were evaluated using rotating disk electrodes in 0.1 M KOH solution and the current density values were consistently higher for Co phthalocyanine based electrodes compared to Fe phthalocyanine. The fuel cell performance of the MEAs with Co

and Fe phthalocyanines and Tanaka Kikinzoku Kogyo Pt/C cathode catalysts were 100, 60 and 120 mW cm^{-2} using H_2 and O_2 gases.

This thesis also includes work on synthesizing nitrogen doped MWCNTs using post-doping and *In-Situ* methods. Post-doped N-MWNCTs were prepared through heat treatment with NH_4OH as nitrogen source. Characterization was done through fuel cell testing, which gave peak power density ~40mW.cm^{-2}. For *In-Situ* N-MWCT, pyridine was used as nitrogen source. The sample characterization was done using Raman spectroscopy and RBS, which showed the presence ~3 at.% of nitrogen on the carbon surface.

DEDICATION

To my parents Syed Jawed Shah and Rehana Shah

ACKNOWLEDGMENTS

I would like to express my sincere gratitude to my graduate committee chair and advisor, Dr. Arunachalanadar Madakannan who always supported and guided me. Due to his continuous encouragement, I was able to complete my research work.

I am grateful to my committee member Dr. Govindasamy Tamizhmani for his great support and guidance during my graduate studies; and also for granting me with a research assistantship.

I am thankful to my committee member Dr. Narciso Macia for his dedication and commendable guidance throughout my thesis work.

I would like to express my gratitude Ivar Kruusenberg and K. Tammeveski from University of Tartu, who provided great help in accomplishing this research work.

I would like to thank my colleagues Anthony Adame, Rashida Villacorta, Aditi Jhalani, Eric Hinkson, Adam Arvay, Yen Huang and Xuan Liu for their encouragement and inspiration.

I appreciate the assistance from Rene Fischer on the facilities of the projects.

I thank Julie Barnes and Martha Benton for their help on preparing my graduation.

I thank all my friends who encourage and supported me during graduate studies.

In the end, I would express my honest gratitude to my parents Syed Jawed Shah and Rehana Shah; and to my siblings Nida Shah, Hira Shah, Irfan Raza Shah and Owais Raza Shah, whose support and encouragement always influenced me to move forward and achieve my goals.

TABLE OF CONTENTS

Page

CHAPTER Page

CHAPTER Page

CHAPTER Page

LIST OF TABLES

LIST OF FIGURES

Figure Page

Chapter 1

INTRODUCTION

1.1. Background

This approach in the automotive market has provided the fuel cell technology to prove itself on commercial Energy from alternative sources such as fuel cells, photovoltaic (solar cells), wind power, biofuels, harnessing waste energies and numerous other technologies; is the only approach which can provide with the solution of clean power generation for various applications. All these technologies are targeting to reduce the carbon foot prints. However, at the same time these energy sources have to compete on the basis of lower cost, simplicity, higher output efficiencies, durability and reliability; with each other and conventional technologies [1].

Among many industries, technical developments in the automobile market throughout the world are increasingly determined by the minimum amount of emissions as well as the type, availability and total consumption of fuel. Therefore, fuel cells can make a breakthrough in this regard, by offering new opportunities, meeting the requirements of resource preservation and emission restrictions.

1.2.What is Fuel Cell?

Fuel cell is an electrochemical device that converts the chemical energy from the fuel (e.g. hydrogen, methanol) and oxygen into electricity and heat. The fact that fuel cell is less pollutant and serves as an alternate source of energy has increased the process of research in this field.

1.2.1 Advantages of Fuel cell

Following are the main advantages of fuel cell as explained in [2]

1. Efficiency: Fuel cells are generally more efficient than combustion engines whether piston or turbine based. Also, small systems can be just as efficient as large ones. This is very important in the case of the small local power generating systems needed for combined heat and power systems.
2. Simplicity: Fuel cell is a very simple technology, with few if any moving parts. This makes fuel cell highly reliable and long-lasting systems.
3. Low emissions: Fuel cells operating on hydrogen are considered as 'zero emission'.
4. Silence: Fuel cells are quiet, which makes them a highly desirable choice for portable and stationary power generation.
5. Renewable fuel source: It is envisaged that as fossil fuels run out, hydrogen will become the major world fuel. It would be generated, for example, by massive arrays of solar cells electrolyzing water.

1.2.2 Working principle

In general a fuel cell is comprised of gas channel plate, gas diffusion layer (GDL) and membrane electrode assembly (MEA) as shown in the figure 1.1. In case of low temperature fuel cells the hydrogen gas is supplied at the anode side while the oxygen/air at the cathode. Hence, the overall reaction is,

$$H_2 + ½\ O_2 = H_2O + \text{Electricity} + \text{Heat} \qquad (1.1)$$

This reaction in the fuel cell gives rise to three phase interface at the membrane electrode assembly (MEA), and plays an important role in the fuel cell design.

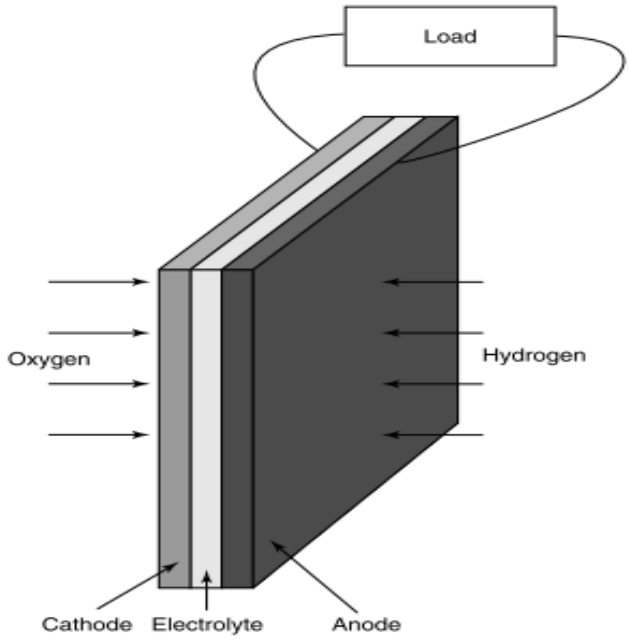

Fig. 1.1: Basic (MEA) construction of a fuel cell [2]

1.2.3. Types of Fuel cells

Fuel cells can be categorized into the following types:

Proton exchange membrane fuel cell (PEMFC)

Alkaline fuel cell or (AFC)

Direct methanol fuel cell (DMFC)

Phosphoric acid fuel cell (PAFC)

Solid oxide fuel cell (SOFC)

Molten carbonate fuel cell (MCFC)

1.2.4. Difference between AMFC and PEMFC

The basic difference between low temperature PEMFC and AMFC is explained below:

a) PEMFC:

PEMFC works on an acid electrolyte. At the anode side hydrogen gas ionizes, releasing electrons and creating H+ ions (or protons), while water is generated at the cathode as shown in the following equations:

$$2H_2 \rightarrow 4H^+ + 4e^- \quad \text{(Anode)} \qquad (1.2a)$$

$$O_2 + 4e^- + 4H^+ \rightarrow 2H_2O \quad \text{(Cathode)} \qquad (1.2b)$$

The electrolyte must only allow H^+ ions to pass through it, and not electrons. Otherwise, the electrons would go through the electrolyte, not a round the external circuit, and all would be lost. Figure 1.2 shows basic PEMFC working.

b) AFC:

AFC woks on Alkaline (OH−) ions electrolyte and has same overall reaction as PEMFC, however, the reactions at each electrode are different as shown in the equations below. At the anode side (OH−) ions react with hydrogen, releasing electrons, and producing water. At the cathode, oxygen reacts and forms new OH− ions. Figure 1.3 shows basic AFC working principle.

$$2H_2 + 4OH^- \rightarrow 4H_2O + 4e^- \quad \text{(Anode)} \qquad (1.3a)$$

$$O_2 + 4e^- + 2H_2O \rightarrow 4OH^- \quad \text{(Cathode)} \qquad (1.3b)$$

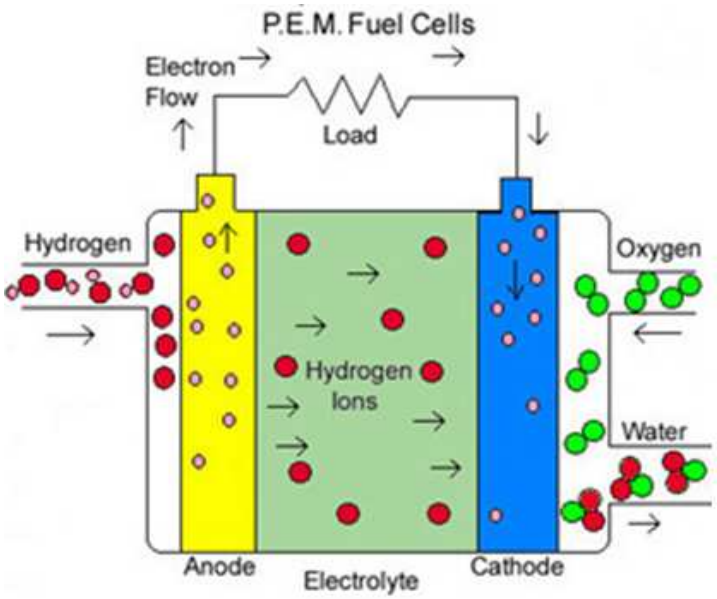

Figure 1.2: PEMFC working principle [4]

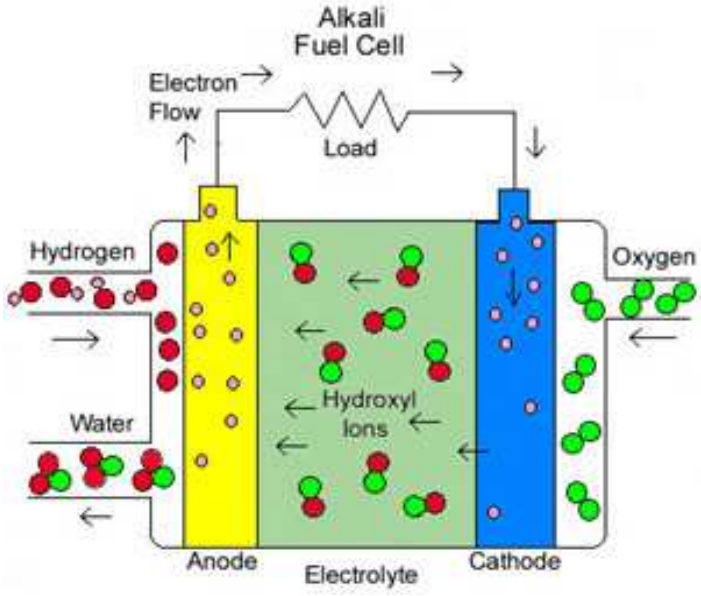

Figure 1.3: AFC working principle [4]

1.2.5. Advantages of AFC over PEMFC:

1. Alkaline fuel cell has a lower activation loss at cathode compared to acid electrolyte fuel cell, due to fast oxygen oxidation rates in AFCs. Therefore, AFCs have higher open circuit voltages than PEMFC.
2. Cost of the AFC systems is much less than PEMFC. This is due AFC's ability to utilize low cost electrolyte (potassium hydroxide) and non-noble metals electrodes.
3. AFC has better theoretical efficiency than that of PEMFC. The electrical efficiency of a typical AFC is ~50%, however, 60% has been achieved by UTC Power, who supplies Alkaline fuel cells to NASA's Space Shuttle Fleet.
4. Finally, AFC systems are found to be less complex than PEMFC, because water management problem is much easily solved.

1.2.6. Types of AFC

AFCs can be widely categorized based on operating temperature and electrolyte type.

1. AFC type based on operating temperature range

Alkaline fuel cells can be categorized into low temperature and high temperature. Low temperature AFCs operate at temperatures as low as 25°C up to 75°C. High temperature AFCs operate at 100°C up to 250°C.

2. AFC type based on electrolyte type

Alkaline fuel cell can further be categorized into following according to the type of electrolyte used:

i) Liquid electrolyte AFC

In this type of fuel cell KOH solution act as mobile electrolyte and is pumped around the fuel cell. Hydrogen and oxygen gases are also circulated. It is the mostly used type of AFC as electrolyte can be replaced when desired.

ii) Static electrolyte AFC

In this type of AFC, KOH electrolyte solution is held within a matrix (usually asbestos).

iii) Solid polymer membrane AFC

Recently a new development has been made in the alkaline fuel cell industry, where liquid electrolyte is replaced with a solid polymer membrane. Alkaline membrane fuel cell (AMFC) uses OH^- based membrane. This invention has provided AMFC with many advantages over conventional liquid electrolyte AFC such as:

a. Liquid electrolyte AFC suffers with the poisoning of KOH electrolyte potassium carbonate as shown in the equation. This is due

to carbon dioxide from the air. CO_3^{2-} ions can reduce the OH^- ion concentration and degrade the performance of AFC.

$$2KOH + CO_2 \rightarrow K_2CO_3 + H_2O$$

b. Also, liquid electrolyte AFC requires extra pumping equipments and later maintenance is needed in case of leakage and corrosion.

c. AMFC is compact and portable.

1.2.7. Fuel cell applications

Fuel cell power covers a wide range of applications, from systems of a few watts up to megawatts; such as from small portable electronics to automotive to large utility power generation systems. Therefore, fuel cells are unique as energy converters. Figure 1.4 and Table 1.1 shows the types, their efficiencies and applications of fuel cells available.

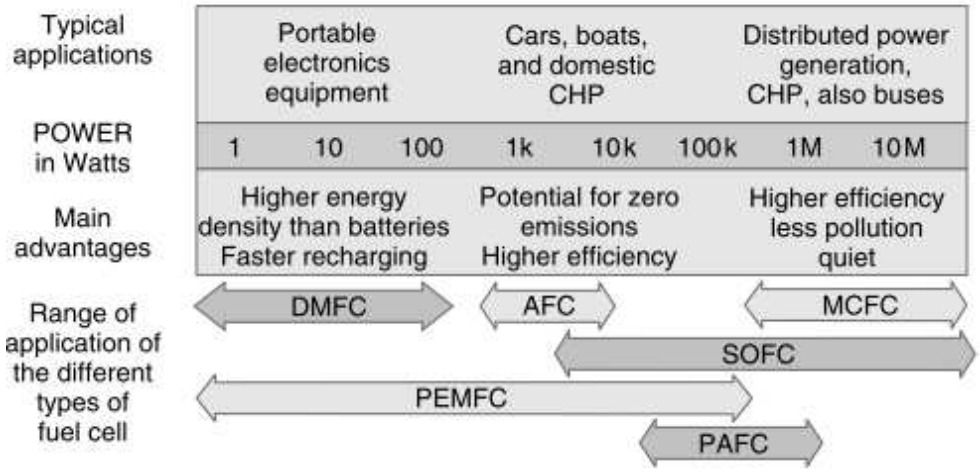

Figure1.4: Application and advantages of different types of fuel cells

Low temperature fuel cells i.e. proton exchange membrane fuel cells (PEMFCs) and alkaline fuel cells (AFCs), operates within 100 °C and catalysts utilization is must for the reaction to occur. High temperature fuel cells usually operate between 200 °C to 800 °C. They do not require any catalyst and utilize higher temperatures for the energy production.

Table 1.1: Fuel cell efficiency, system output and application

Fuel Cell Type	Mobile Ion	Operating Temperature	System Output	Electrical Efficiency	Applications
Proton Exchange Membrane (PEMFC)	H^+	30-100°C	≤ 1kW-250kW	25-58%	Backup power, Portable power, Transportation
Alkaline (AFC)	OH^-	50-200°C	10kW-1MW	60%	Military, Space
Direct Methanol (DMFC)	H^+	20-90°C	≤100kW	35-40%	Low power portable electronics
Phosphoric Acid (PAFC)	H^+	220°C	50kW-1MW	>40%	Distributed generation
Molten Carbonate (MCFC)	CO_3^{2-}	650°C	≤1kW-1MW	45-47%	Electricity utility, Large distributed generation
Solid Oxide (SOFC)	O^{2-}	500-1000°C	≤1kW-3MW	35-43%	Auxiliary power, Electric utility

1.3.Statement of problem

High cost is the main problem in the commercialization of fuel cell technology. It is reported that in general ~55% of the total (PEM) fuel cell cost comprise of electrode [3], because of using Pt catalyst that is very expensive with

limited reserves of only $20ft^3$ [5]. However, this issue can be addressed by using AFC where non-noble catalyst can work really well due the alkaline nature of the electrolyte, as kinetics of oxygen reduction in alkaline media is much faster than in acid media [2].

AFC are widely being operated with liquid alkaline electrolyte as KOH, which can easily be poisoned through carbon dioxide gas from air [6]. This problem is solved by employing solid alkaline membrane as electrolyte.

It is also known that apart from non-noble metals, nitrogen doped carbon nanotubes also provide with the great possibility to be used as non-noble metal free catalysts for AFC.

In this study work is done on developing alkaline membrane fuel cell; and identifying and synthesizing low cost cathode catalysts materials:

1. The first task of this thesis is to identify the optimum operating conditions for solid polymer alkaline membrane fuel cell.
2. Developing low cost, non-noble catalysts supported on MWCNT was the second task of this thesis.
3. Finally, work is also done on synthesizing N/MWCNT (post-doped) for cathode catalyst and N/MWCNT (In-Situ) for GDL.

X-ray photoelectron spectroscopy (XPS) and rotating disk electrode (RDE) were used for non-noble catalyst characterization. Raman spectroscopy and Rutherford backscattering spectroscopy (RBS) were used to characterize In-Situ N/MWCNTs. Fuel cell performance evaluation was carried out as well by using fuel cell testing station.

1.4.Scope of Work

Following are the objectives that were achieved through this thesis work:

1. Indentifying optimum operating conditions and MEA fabrication for AMFC by:
    a. Identifying proper composition of OH^- ionomer and catalyst for AMFC ink preparation and electrodes fabrication.
    b. Analyzing and identify optimum temperature and humidity conditions for alkaline solid polymer membrane.
2. Developing and characterizing transition metal macrocycle based catalysts (CoPc and FePc)
    a. Functionalizing multi-walled carbon nanotubes for CoPc and FePc support.
    b. Synthesizing CoPc/MWCNT and FePc/MWCNT catalysts by pyrolysis.
    c. Characterization of CoPc/MWCNT and FePc/MWCNT catalysts by RDE, XPS and fuel cell testing.
3. Synthesizing and characterizing N doped MWCNT materials
    a. Synthesizing N/MWCNT (as cathode catalyst) through post-doping using NH_4OH and characterizing by fuel cell testing.
    b. Synthesizing In-Situ N/MWCNT (as GDL) through CVD using pyridine as nitrogen source. Characterization was done by Raman spectroscopy and RBS.

To the author's knowledge, there is no literature on the alkaline fuel cell studies performed with CoPc and FePc modified MWCNTs. In this study FePc/MWCNT and CoPc/MWCNT electro-catalysts have been synthesized as alternative cathode materials to Pt/C in alkaline fuel cell using Tokuyama A201 membranes. The electrocatalytic activity of FePc/MWCNT and CoPc/MWCNT modified glassy carbon electrodes towards oxygen reduction using the rotating disk electrode (RDE) method is also explored.

1.5. Organization of Thesis

This thesis consists of five chapters

1. Chapter 1 is the introduction of fuel cells and includes a brief background, statement of problem and scope of work.
2. Chapter 2 discusses literature review and discusses the history and development of fuel cells, their types, difference between PEMFC and AMFC, potential application of alkaline fuel cells, transition metal (TM) macrocyclic-catalysts for AMFC and N doped MWCNT.
3. In Chapter 3 explains experimental section in detail for synthesizing and characterizing TM catalyst materials and N doped MWCNTs.
4. Chapter 4 provides with the results and discussion by comparing cost and performance of Pt/C with non-noble catalysts in AMFC.
5. Chapter 5 is the last chapter which concludes all the findings from this thesis work.

Chapter 2

LITERATURE REVIEW

2.1. History and development of Hydrogen fuel cell

Fuel cells are one of the oldest energy conversion technologies [7]. The first demonstration of a (PEM) fuel cell was by lawyer and scientist William Grove in 1839 [8].

2.1.1. PEMFC History

The proton exchange membrane fuel cell (PEMFC) was first developed by General Electric in the United States in the 1960s. This was used by NASA on their first manned space vehicles. The development in the PEMFC was initiated once again by Ballard power systems in early 1990s. Currently, PEMFCs are the one of the most widely manufactures and used low temperature fuel cells.

2.1.2. AFC History

Alkaline fuel cells (AFC) were first described in the year 1902; however, it was between 1940s and 1950s that F.T. Bacon at Cambridge proved AFCs as practical power units. Alkaline fuel cells were used for the Apollo missions, which took man to the moon. The success of the alkaline fuel cells in this application, and the demonstration of high power working fuel cells by Bacon, led to a good deal of experiment and development of alkaline fuel cells during the 1960s and early 1970s. Demonstration alkaline fuel cells were used to drive agricultural tractors, provide power to offshore navigation equipment and boats, drive fork lift trucks, and so on [2].

2.2. Fuel cell components

Following are the major components of low temperature fuel cells (PEMFC/AMFC). Figure 2.1 shows in detail the arrangement of these components.

1. Bipolar plates: They contain flow channels for the fuel reactants (O_2/Air and H_2). Bipolar plates are used to interconnect the fuel cells together into stack.
2. Membrane electrode assembly (MEA): MEA consists of catalyst layer for anode and cathode electrodes. The catalyst is sprayed or printed on the ion conducting membrane. Membrane is a solid polymer electrolyte which is defined as Nafion membrane (proton conducting) for PEMFC and OH^- membrane (anion conducting) for AMFC. Proper MEA fabrication is the heart for efficient fuel cell performance.
3. Gas diffusion layer (GDL): GDL plays very important role in fuel cell. It consists of carbon fiber or woven cloth macroporous layer. The fuel enters through GDL which facilitates conduction of electrons to and from the catalyst layer. It also provides mechanical support to the structure. It is responsible for the water management, which is very crucial in determining stability and performance of low temperature fuel cells.

Fuel cells have very few moving parts; however in case of combined heat and power (CHP) system it might require heat exchanger. Apart from this other

components like humidifiers, pumps, power electronics, compressors are also used, and these are called balance of plant (BOP).

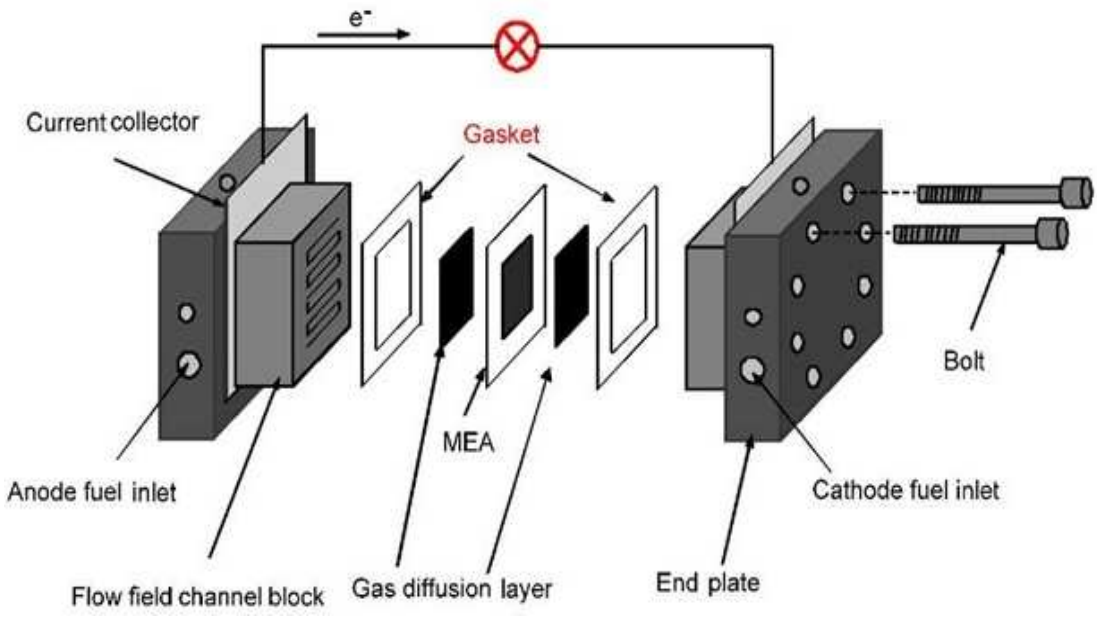

Figure 2.1: Arrangement of low temperature fuel cell components [9]

2.3. Performance losses in fuel cell

In order to fully understand the performance of fuel, it is important to know the different loss regions of polarization curve. From Figure 2.2 it can be seen that the open circuit voltage (OCV) is less than the theoretical value, there is a rapid initial fall in voltage. The voltage then stabilized and become more linear. It is also shown that at higher current densities there is a sudden voltage drop.

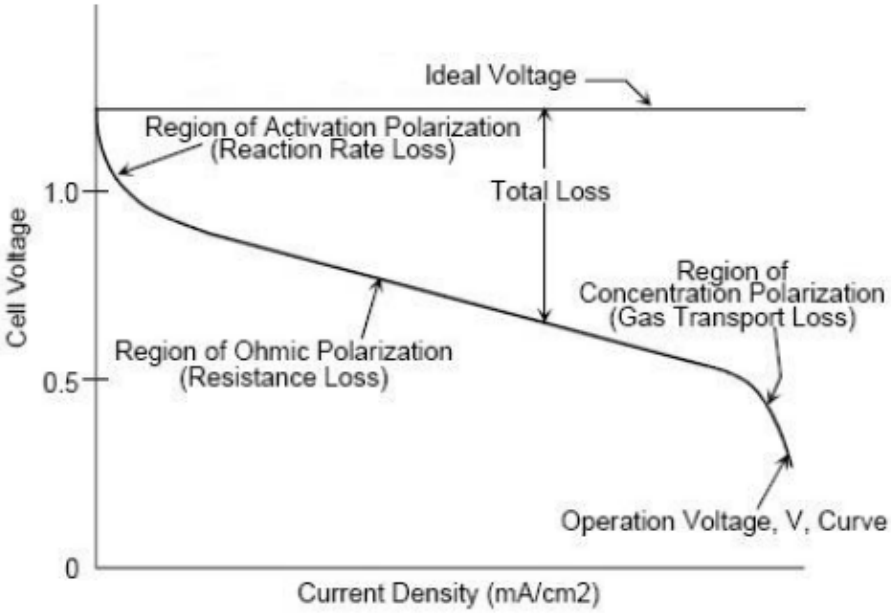

Figure 2.2: Voltage drops in low temperature fuel cell [10]

Following are the different losses that influence performance of fuel cell

a. Activation loss: This loss causes the initial drop in the voltage and is due to the reaction sluggishness at the surface of electrodes.

b. Fuel crossover and internal currents loss: When electrolyte conducts electrons and waste energy by allowing fuel to pass through it; which cause loss due to fuel cross over and internal currents.

c. Ohmic loss: This is IR drop; and is caused by the resistance to the flow of electrons through the electrodes and interconnections. The resistance in the electrolytes to the flow of ions also results in ohmic losses.

d. Mass transport or concentration loss: This results from the change in concentration of the chemical reactants at the surface of the electrodes as the fuel is used.

2.4. Technical Limitations

The technical limitations such as high cost, durability and reliability problems, and fuel (generation, storage and delivery) must be overcome by fuel cells, in order to become commercially available. Following points discusses these issues in detail, while figure 2.3 presents jigsaw puzzle diagram for these limitations, which need to be solved by FC industry and researchers.

a) Cost: The major technical problem for fuel cell in becoming commercially available is its high cost, which is mostly due to the expensive catalyst materials used (in low temperature fuel cell). In order, to be competitive with ICE (Internal combustion engine) and stationary power generations systems, fuel cell cost must be reduced; by using alternative cheap materials and construction methods.

b) Durability and reliability: The fuel cell technology must be highly reliable and durable to compete with its counter parts. According to ICE standards automotive fuel cell must perform ~ 5500 h and stationary fuel cell must provide a steady operation for ~50000 h. However, fuel cell is found to degrade in its performance with time due to a variety of phenomena.

c) System size: Fuel cell systems must be compact, light weight and highly efficient. For this reason US DOE has targets for system power density and specific power.

d) Air, thermal and water management: Proper water management is very crucial from fuel cell operation respect. When fuel cell is used for automotive purpose these issues like thermal and air management also

need to be taken into account. Appropriate cooling and heating systems must be used.

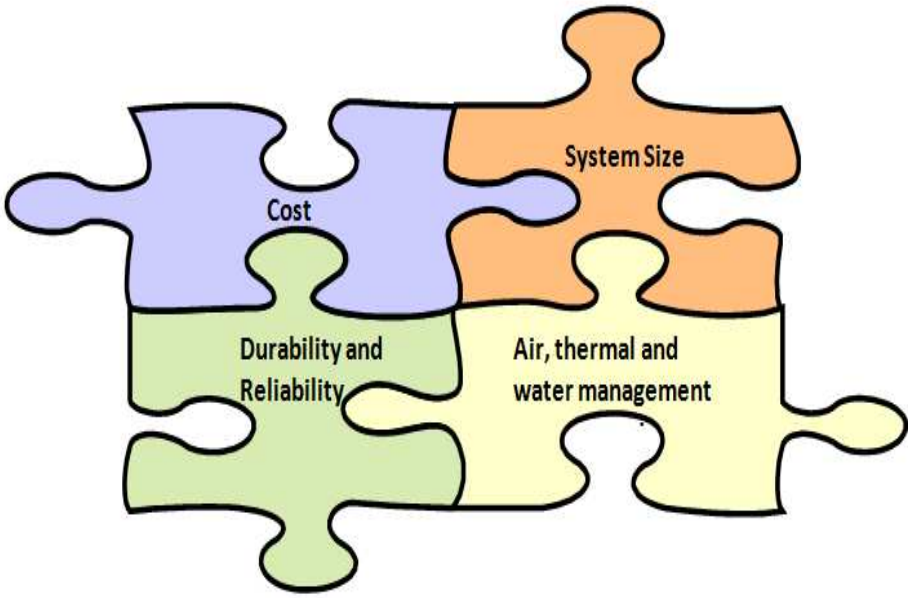

Figure 2.3: Fuel cell technical limitations

2.5. Catalysts for fuel cell

2.5.1. Why catalyst is required?

Due to strong O=O bond (498 kJ mol $^{-1}$) the oxygen reduction reaction (ORR) rate is very slow[11], therefore higher amount of noble metal catalyst is required specially at the cathode of fuel cell. In general, the ORR catalyst materials are Pt or Pt-transition metal alloys on carbon or multi-walled carbon nanotubes in the low temperature fuel cells [12- 14].

2.5.2. Transition metal (TM) macrocyclic-catalysts for AFC

In the cost point of view there is a huge interest in developing fuel cell electrodes with lower amount of noble metal catalysts or non-noble metal catalysts [12,15- 22] towards ORR.

Transition metal (TM) macrocycles are one of the many different non-noble metal catalysts that are actively researched both in fundamental studies and in practical applications. The most common TM macrocycles studied are TM porphyrins and their analogues: TM tetraphenyl porphyrins (TM TPP's) and TM phthalocyanines (TM Pc's). These types of TM macrocycles have been investigated mainly as efficient ORR catalysts [23].

Iron phthalocyanines (FePc), cobalt phthalocyanines (CoPc) and other similar M-N_4-macrocycles supported on different carbon nanomaterials have attracted much attention towards ORR in alkaline medium since the pioneering work of Jasinski [24]. It is worth mentioning about the recent reports on various non-noble metal catalysts studied towards ORR [25-31]. Nitrogen containing transition metal catalysts have been used for oxygen reduction both in acid [26,28,29] and alkaline media[31].

2.5.3. Carbon nanotubes (CNTs) as catalyst-support

Carbon nanotubes (CNTs), Ketjen Black and Vulcan carbon serves as good catalyst support and have been employed for FePc and CoPc complexes in numerous studies in the field of oxygen reduction electrocatalysis [32-36]. There are different types of CNTs available such as single walled and multi-walled CNTs. Figure 2.4 show these different types of CNTs.

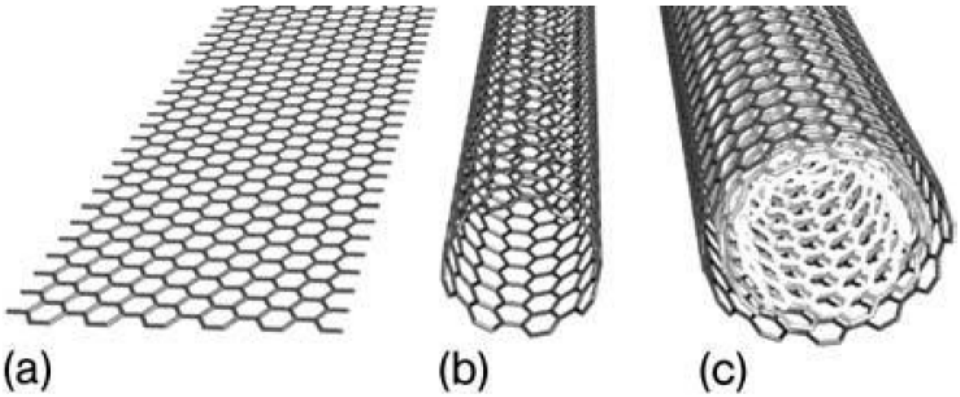

Figure 2.4: Different types of carbon nonotube structures (a) Structure of single layer graphite (b) Single walled carbon nanotube (c) Three layered multi walled carbon nano tube [33]

In this thesis MWCNTs were used as a catalyst support material due to their exceptional properties as mentioned below [33]:

1. Higher Mechanical strength (100x strength of steel)
2. Electrical conductivity of Cu
3. 3x thermal conductivity of diamond
4. Larger Surface Area
5. Better Oxidative Stability and accessibility for O_2 molecules

Functionalizing MWCNTs with phthalocyanines was reported to improve the electrocatalytic properties of these complexes. Phthalocyanines adsorb strongly on CNTs via noncovalent $\boldsymbol{\pi}$- $\boldsymbol{\pi}$ interactions and form "molecular phthalocyanine electrodes" [34]. Different research groups have reported achievements in enhancing the electrocatalytic activity as well as stability of CoPc/Vulcan and CoPc/CNT materials by pyrolysis in inert atmosphere [37, 38]. The stability of the catalysts is improved by a heat-treatment.

2.5.4. Comparison of FePc/MWCNT and CoPc/MWCNT catalysts with Pt/C

Besides higher cost of Pt catalyst is reported to be effected by drawbacks that can be addressed using FePc and CoPc. For example Pt catalysts undergo $2e^-$ ORR, which not only reduces the efficiency of the system but hydrogen peroxide produced during reaction can degrade the catalytic activity of catalysts [39]. The H_2O_2 radicals also attack the catalyst carbon layer and the proton exchange membrane, resulting in significant fuel cell degradation, and even failure. However, it has been reported that FePc and CoPc have the ability to promote the $4e^-$ oxygen reduction to water without the formation of peroxide intermediates [29,40,41].

2.6. Solid polymer membrane for AFC

With the possibility of using non-noble metal catalysts for ORR in the alkaline fuel cells, there is a renewed interest in using anion exchange membrane electrolyte, as reported in detail in a review [41]. Very recently, polymer electrolytes based on polyphenylene oxide, polyxylylene block ionenes, PVA, polysulfone have been studied in alkaline system very successfully [42-47]. Li et al. have reported using Tokuyama anion exchange membrane with Co-Fe alloy cathode catalyst for alkaline fuel cells [30].

2.7. N doped MWCNT for AFC

Carbon nanotubes (CNTs) are promising material for fuel cell applications; due to their high chemical stability and good electric conductivity. Studies have also shown that the doping of CNTs with various elements such as

nitrogen (N), potassium (K) or boron (B) is a significant and effective technique to modify both chemical and electronic properties of CNTs [48].

2.7.1. Nitrogen doped CNT's effectiveness as ORR

It is very important to search for a low-cost, stable and more active electrocatalysts for the ORR in alkaline medium. Therefore, modifying CNTs by introducing different nitrogen functional groups can be use to enhance their electrocatalytic activity for the ORR [48].

It is believed that in nitrogen-containing carbon material, pyridinic or pyrrol/pyridone type nitrogen is responsible for the enhanced ORR activity. It is also reported that pyridinic nitrogen possesses one lone pair of electrons (in addition to the one electron donated to the conjugated bond), facilitates the reductive oxygen adsorption and eliminates H_2O_2 formation [49, 50, 51]. By using heat treatment technique the nitrogen functional groups transform to more thermally stable structure. Furthermore, nitrogen is known to create defects on carbon, which may then increase the edge plane exposure and thus (pyridinic type nitrogen) enhance the catalytic activity [48].

2.7.2. Preparation of N doped MWCNTs

N doped MWCNT can be achieved either in the form of In-Situ N-MWCNTs or through post-doping method. It is reported that different available nitrogen functional groups can be doped on the MWCNT surfaces by varying the synthesis procedure, amount of nitrogen source and the process parameters [51-55]. In general, chemical doping with N or B is considered an effective method to intrinsically modify the properties of carbon materials. Especially nitrogen doping

plays a critical role in regulating the electronic and chemical properties of carbon materials due to its comparable atomic size and five valence electrons available to form strong valence bonds with carbon atoms[56].

2.8. AFC as a promising power source for future

AFC can use various forms of fuel sources and catalysts unlike PEMFC, which provide it with lots of research opportunities in future. AFC can utilize numerous fuel sources, as [57] reported to employ formate salts as anode fuel for AMFCs as in direct formate fuel cells. Formate salts have advantage of being non poisonous, renewable, portable and low cost. Moreover, alkaline fuel cells have huge potential to utilize wide variety of organic catalysts, which are very cheap and renewable. For example, effective performance of urea and waste water (in urine fuel cells) as electrodes for AFC is reported [58]

Chapter 3

EXPERIMENTAL[1]

In this thesis, work has been carried out for the development of low cost efficient catalyst materials for the alkaline membrane fuel cells. It mainly discusses the following topics:

1. Identifying the optimum operating conditions for the AMFC.
2. Development of MWCNT supported transition metal (TM) macrocycle electrocatlysts.
3. Synthesizing of N doped MWCNTs.

3.1. Optimization of fuel cell performance parameters

In this thesis, several parameters were studied during the experimental procedures for identifying optimum performance, suitable for solid polymer alkaline membrane (as its properties differ from Nafion membrane). The fuel cell testing system as shown in figure 3.1 was utilized to accomplish this task. Parameters studied are described below:

1. Various samples of (FePc or CoPc)/ MWCNT catalysts were studied. The samples contained different (FePc or CoPc)/ MWCNT wt% ratios; namely 50/50, 25/75 and 75/25. The best results were achieved from 50/50 sample
2. Pyrolysis was done at two different temperatures of 600 $^{\circ}$C and 800 $^{\circ}$C. Optimum performance was observed in the 800 $^{\circ}$C sample through fuel cell testing

3. Optimum MEA fabrication and testing conditions (temperature and humidity) were found for the AMFC

However, this thesis only discusses the samples that were identified to give optimum performance in AMFC.

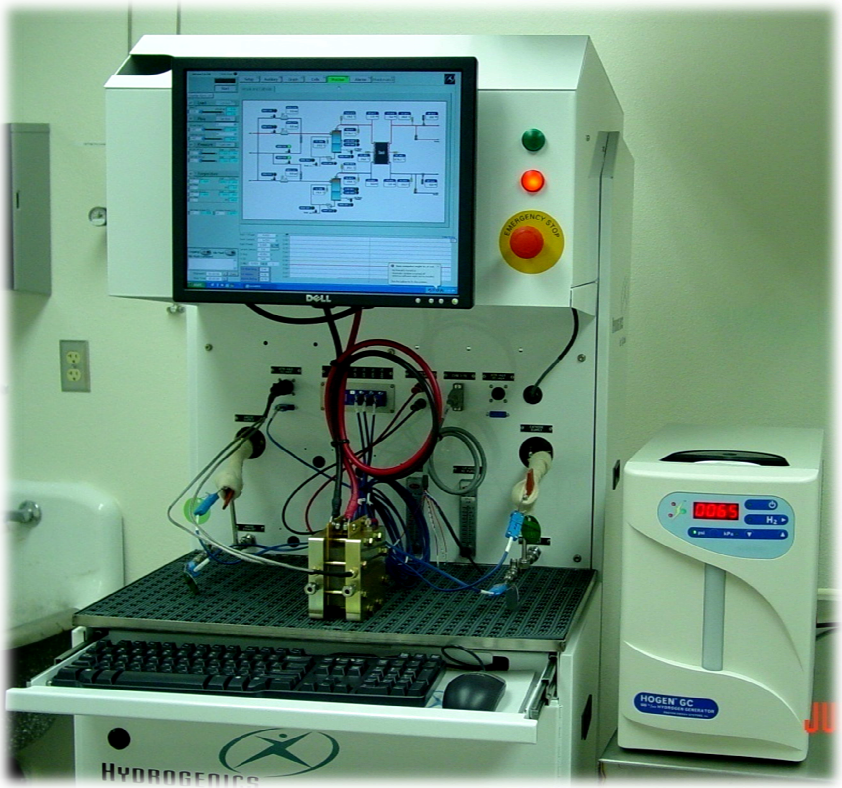

Figure 3.1: Fuel cell testing system

[1] This experimental method is based on the published paper: Kruusenberg, I., Matisen, L., Shah, Q., Kannan, A. M., & Tammeveski, K. (2011). Non-platinum cathode catalysts for alkaline membrane fuel cells. *International Journal of Hydrogen Energy*.nano electrocatlyst

3.2. Preparation of FePc/MWCNT and CoPc/MWCNT electrocatalysts

3.2.1. Materials

The iron (II) phthalocyanine (FePc) and cobalt (II) phthalocyanine (CoPc) were purchased from Sigma Aldrich. The multi-walled carbon nanotubes (MWCNTs, purity >95%, diameter 30±10 nm, length 5-20 mm) used were purchased from NanoLab, Inc. (Brighton, MA, USA). 20 wt.% Pt commercial catalyst supported on Vulcan XC-72 was purchased from E-TEK, Inc. (Frimingham, MA, USA) and commercial 46.1 wt.% Pt catalyst supported on Ketjen Black was purchased from Tanaka Kikinzoku Kogyo K.K. (Japan). Anion exchange membrane (model # A201) samples were provided by Tokuyama (Tokuyama Corporation, 2-1, Kasumigaseki3-chome, Chiyoda-ku, Tokyo 100-8983, Japan). The characteristics of the membrane are given in Table 3.1. A 5 wt.% OH^- ionomer solution (Tokuyama) was used in the preparation of catalyst ink in water. All the solutions were prepared with Milli-Q water (Millipore, Inc.).

Table 3.1: Properties of Tokuyama anion exchange membrane (#A201)

Parameter	Value
Thickness (μm)	28
Ion exchange capacity (mmol g^{-1})	1.8
Water content (%)	25
Ionic conductance at 23 ^oC, 90% RH (mS cm^{-2})	11
Ionic conductivity 23 ^oC, 90% RH (mS cm^{-1})	42
Burst strength (Mpa)	0.4
Dimensional change: wet to dry (%) (a) MD (b) TD	 2 4

3.2.2. Experimental procedure

In order to disperse the catalyst on the surface of MWCNTs, a mixture of 200 mg FePc or CoPc and 200 mg MWCNTs in 40 ml isopropanol was prepared and sonicated for 30 min followed by magnetic stirring for 1 h. The homogeneous mass was placed in a ceramic boat, vacuum dried at 100°C and pyrolysed at 800°C for 2 h in flowing argon atmosphere. The initial loading of FePc or CoPc on the MWCNTs was 50 wt.% and the final loading was not ascertained. Flow chart diagram in figure 3.2 demonstrate the step by step procedure from catalyst preparation.

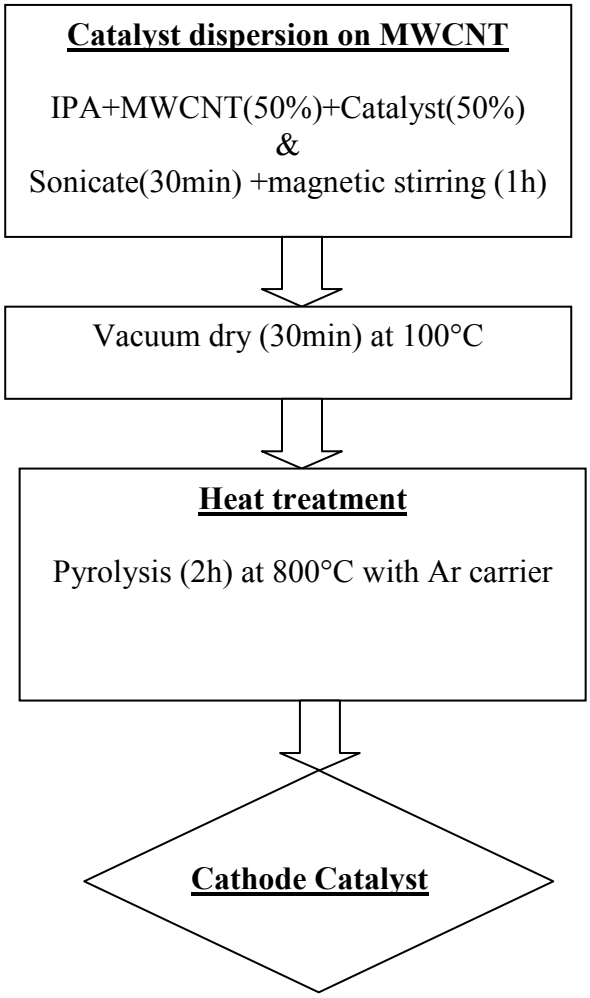

Figure 3.2: Flow chart diagram for catalyst preparation

3.3.Characterization of FePc/MWCNT and CoPc/MWCNT electrocatalysts

Following methods were employed for the characterization purpose of the TM electrocatalyst samples

1. X-ray photoelectron spectroscopy (XPS)
2. Rotating disk electrode (RDE)
3. Fuel cell testing

3.3.1. X-ray photoelectron spectroscopy analysis

The surface composition of the as-received MWCNT, FePc/ MWCNT and CoPc/MWCNT materials was analyzed using X-ray photoelectron spectroscopy (XPS). For the XPS studies the catalyst materials in isopropanol (1 mg ml^{-1}) were deposited on a glassy carbon plate (1.1 x 1.1 cm) and the solvent was allowed to evaporate in air. The XPS measurements were carried out with a SCIENTA SES-100 spectrometer using an unmonochromated Al Kα X-ray source (incident energy=1486.6 eV), a takeoff angle of 90° and a source power of 300 W. The pressure in the analysis chamber was below 10^{-9} Torr. While collecting the survey scan, the following parameters were used: energy range = 800 to 0 eV, pass energy = 200 eV, step size = 0.5 eV and for the high resolution scan: energy range = 420-395 eV for the N1s region; 740-700 and 800-775 eV for the Fe2p and Co2p regions, respectively with pass energy = 200 eV and step size = 0.1 eV.

3.3.2. Electrode preparation for RDE measurements and electrochemical characterization

For the rotating disk electrode (RDE) experiments a glassy carbon (GC) disk of geometric area (A) of 0.2 cm^2 was used as substrate material. GC disks were pressed into a Teflon holder and then electrodes were polished to a mirror finish with 1 and 0.3 mm alumina slurries (Buehler). After alumina polishing the electrodes were sonicated in water for 5 min. To obtain a uniform layer of electrocatalyst onto GC surface, the electrodes were modified with different catalysts using aqueous suspensions (1 mg ml^{-1}) containing 0.5% OH^- ionomer solution. All the suspensions were sonicated for 1 h. Then a 20 ml aliquot of prepared catalyst suspension was pipetted onto GC surface and was allowed to dry in ambient air for 24 h.

The electrochemical measurements were made using the RDE technique employing an EDI101 rotator and a CTV101 speed control unit (Radiometer). Experiments were controlled with the General Purpose Electrochemical System (GPES) software and the potential was applied with an Autolab potentiostat/galvanostat PGSTAT30 (Eco Chemie B.V., The Netherlands). A Pt foil served as the counter electrode and a saturated calomel electrode (SCE) was used as a reference. All the potentials are referred to this electrode. Electrochemical experiments were carried out in 0.1 M KOH solution at room temperature (23 ± 1°C). The solutions were saturated with Ar (99.999%, AGA) or O_2 (99.999%, AGA). A continuous flow of gases was maintained over the solution during the electrochemical measurements.

3.4.Electrode fabrication and performance evaluation for AMFC

Membrane-electrode assemblies (MEAs) were fabricated with commercial carbon-supported Pt catalyst (Pt/C) as anode catalyst and FePc/MWCNT, CoPc/MWCNT and commercial catalyst (Pt/C) on cathode sides of the Tokuyama polymer membrane (A201 membrane, Tokuyama Corporation, Japan). Catalyst ink was prepared by adding Milli-Q water to catalyst material (2 ml for 100 mg of electrocatalyst). In order to extend the reaction zone of the catalyst layer, 5 wt.% ionomer (AS4 ionomer, Tokuyama Corporation, Japan) dispersion (0.8 ml for 100 mg of electrocatalyst) was added to the catalyst slurry. Catalyst layer was coated on the alkaline membrane with 5 cm^2 geometrically active area applying the catalyst ink by spraying method on both sides of the membrane and vacuum dried at 70°C for 15 min. The catalyst loadings were about 0.4 and 0.6 mg cm^{-2} on the anode and cathode sides, respectively.

The MEA was assembled by sandwiching the catalyst coated membrane inside the test cell (Fuel Cell Technologies Inc, Albuquerque, NM, USA) with gas diffusion layers (fabricated by a wire rod coating method [60]) on both sides. Gas sealing was achieved using silicone coated fabric gasket (Product # CF1007, Saint-Gobain Performance Plastics, USA) and with a uniform torque of 0.45 N.m. The single cell fuel cell performance was evaluated with humidified (100% RH) H_2 and O_2 gases at 45°C using Greenlight Test Station (G50 Fuel cell system, Hydrogenics, Vancouver, Canada). The flow rates were fixed at 200 and 400 SCCM for H_2 and O_2, respectively. Figure 3.3 show various procedural steps involved in the fabrication, assembling and testing of fuel cells.

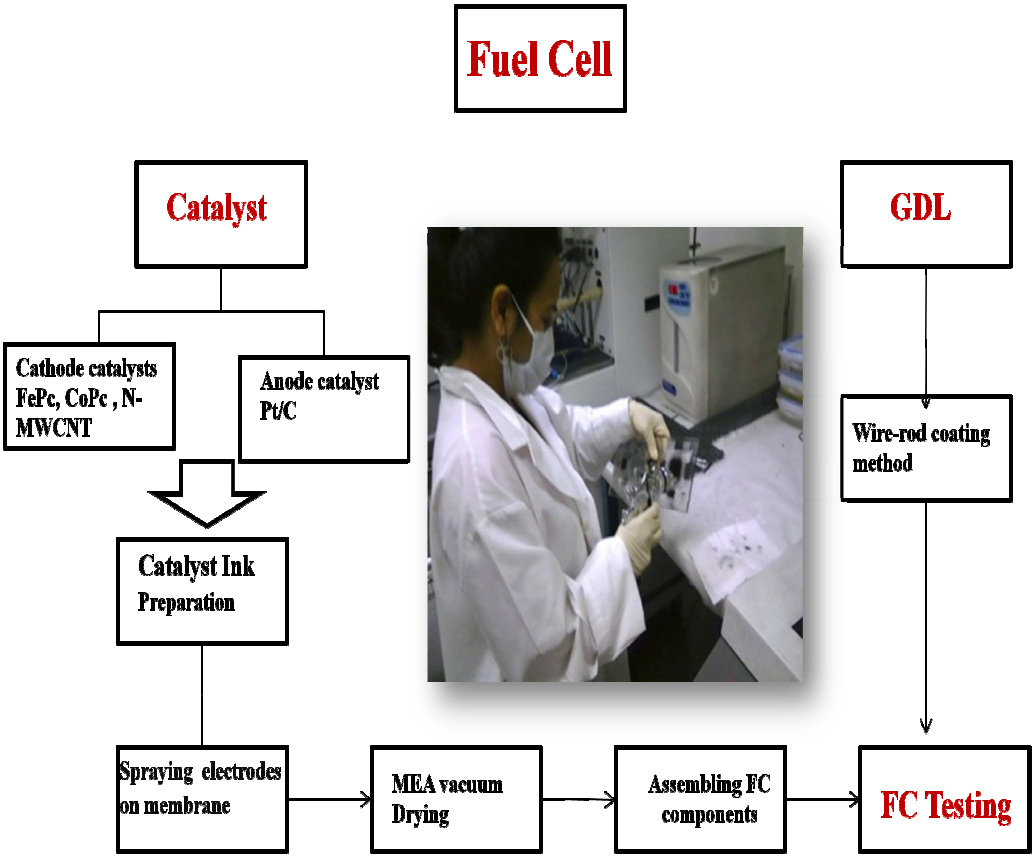

Figure 3.3: Various procedural steps for fuel cell fabrication and testing

3.5. Methods to synthesize CNTs

Chemical vapor deposition process was used for synthesizing and doping CNTs. Nitrogen based carbon nanostructure materials were synthesized in two ways as described below

1. Doping directly during the synthesize of porous multi walled carbon nanotube materials, i.e. ‘‘In-Situ’’ doping; and

2. Post-treatment of pre-synthesized multi walled carbon nanotube materials with nitrogen-containing precursor (NH_4OH, N_2, NH_3 etc.) i.e. post-doping.

3.6.Chemical vapor deposition (CVD) process

Arrangement for the experimental setup for the chemical vapor deposition process is shown in Figure 3.4. Following points briefly describes the function of CVD components:

1. Syringe carrying catalyst solution is placed onto the syringe pump, which pass the controlled amount of liquid catalyst into the furnace.
2. Flow meter is use to maintain proper flow of (carrier gas) Argon.
3. Pre-heater is use for heating the catalyst (carbon/nitrogen source) before it enters into the furnace.
4. Samples used in chemical vapor deposition process are placed in the 3" quartz tube, which is held within the furnace.
5. The liquid residue is collected by the filter flask placed at the end of furnace.

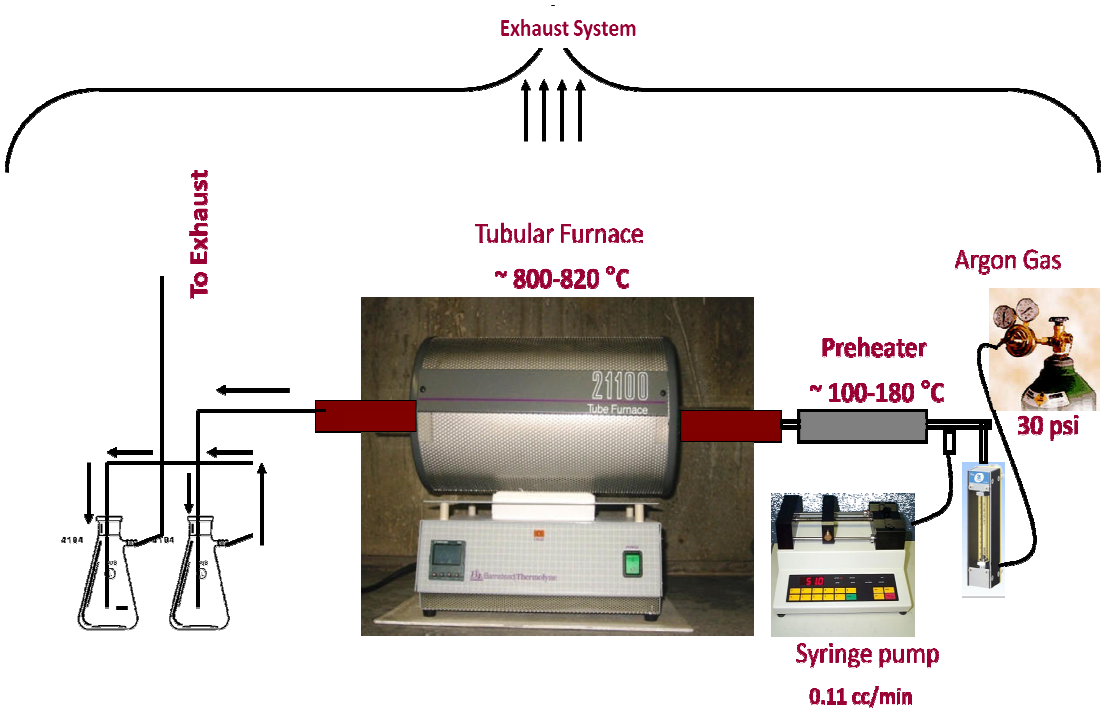

Figure 3.4: CVD experimental setup for synthesizing multi walled carbon nanotubes

3.7. Synthesize of Nitrogen doped MWCNT elctrocatalysts

3.7.1 Materials

In order to grow MWCNT and N/MWCNT, Teflon free carbon paper was obtained from Hollingsworth and Vose Company (West Groton, MA), Aeroxide TiO_2 P25 from Evonik industries (NJ, USA), Pyridine from MP Biomedicals and ammonium hydroxide (50% v/v aq. solution) from Alfa Aesar.

3.7.2. Surface modification of carbon paper

Teflon free and non woven carbon paper with thickness of 0.21 mm was selected to ensure the proper nanotubes growth as Teflon might hinder the catalyst absorption into the carbon paper pores (mean flow pore diameter = 33 µm).

Titanium dioxide (TiO_2) coating is used as a support layer for growing MWCNTs and for the surface modification of carbon paper. TiO_2 coating was prepared by using 200mg of TiO_2 and 10ml of isopropanol alcohol (IPA). The mixture was sonicated for 10minutes. TiO_2 layer was then deposited uniformly on the 2.5cm x 2.5cm Teflon free carbon paper through micro spraying. The sample was then vacuum dry at 60°C for 15 minutes and then placed in the CVD furnace.

3.7.3. Experimental procedure

The experimental procedure for CVD process is described as follows:

1. The sample to be processed is placed at the center of CVD furnace, approximately at a distance of 21cm from the front side of furnace with sample aligned horizontally;
2. Both the ends of quartz tube are fitted carefully using small amount of grease to avoid any gas leakage;
3. Now in order to create inert atmosphere inside the furnace Argon gas is passed at 30 psi, 500 SCCM for about 15 minutes;
4. The furnace is then switched on and set temperature. When the furnace reached stable temperature the pre-heater is switched on to desired temperature;
5. Place the syringe in the syringe pump and connect it to the furnace;
6. Make sure that the flow rate for catalyst in the syringe is 0.11 cc/min with a minimum process time of 40 minutes to obtain optimum results;
7. Furnace is allowed to cool at a temperature of about 200° C before taking out the sample.

For synthesizing different types of CNTs; catalysts (source) and experimental conditions are varied as shown in Table 3.2.

Table 3.2: Catalyst composition and process conditions for synthesizing various MWCNT

Type of MWCNT	Catalyst composition	Process time	Furnace temperature	Pre-heater temperature
1. In-Situ MWCNTs	Xylenes = 10ml Ferrocene=500mg	40mins-1hr	820°C	180-190°C
2. In-Situ N-MWCNTs	Pyridine = 7ml Ethanol = 3ml Ferrocene=500mg	40mins-1hr	820°C	170-180°C
3. Post-doped N-MWCNTs	MWCNT=200mg NH_4OH = 20ml	2hrs-3hrs	800°C	100-120°C

3.8. Characterization of Nitrogen doped MWCNT

The In-Situ N-MWCNTs grown onto carbon paper were characterized through following ways:

1. Raman Spectroscopy;
2. Rutherford backscattering spectroscopy (RBS)

Post-treated N-MWCNT nano elctrocatalysts were characterized by:

1. Fabricating N-MWCNT nano elctrocatalysts as a cathode side in MEA of AMFC. Performance was evaluated through fuel cell testing, under the same conditions as described in section 3.3.3.

3.8.1. Raman Spectroscopy

The Raman data were collected using a custom built Raman spectrometer in 180° geometry. The sample was excited using a 0.65 mW Compass 532 nm laser. The laser power was controlled using neutral density filters. The laser was focused onto the sample using a 50X super long working distance Mitutoyo objective with a numerical aperture of 0.42. The signal was discriminated from the laser excitation using a Kaiser Laser band pass filter followed by a Semrock edge filter. The data were collected using Acton 300i spectrograph and a back thinned Princeton Instruments liquid nitrogen cooled CCD detector.

Raman spectroscopy is one of the methods largely used for determining the degree of structural ordering or the presence of defects in graphitic-like materials. Also in Raman spectra, the ratio of D and G band intensities (I_D/I_G) is used as a diagnostic tool for check.

3.8.2. Rutherford backscattering spectroscopy (R B S)

In Rutherford backscattering spectroscopy (R B S) ~ 4 MeV ^{4}He ions beams were used for detecting the presence of Nitrogen in the N-MWCNT sample. RBS was conducted for MWCNT samples for comparison purposes. RBS also identifies the atomic percentage of various materials composing the N-MWCNT sample.

Chapter 4

RESULT AND DISCUSSION[1]

4.1. Optimization of AMFC performance parameters

Peak performance of AMFC is highly dependent on its operating conditions and proper MEA fabrication.

4.1.1. Effect of temperature on AMFC performance

The effect of temperature on current density in the alkaline membrane fuel cell is described in Table 4.1. Here temperature dependence of current density in AMFC using Pt/C catalyst and H_2/O_2 (Base line Data) was performed. It was observed that current density increased as the temperature increased until 45°C and 100% relative humidity. At these conditions, maximum current density was achieved and AMFC operation was found to be very stable. This optimum current is referred as 100% in the table 4.1. For the temperatures above 45°C, decrease in performance was seen and cell became unstable as well. Relative humidity was decreased to check if poor water management of membrane is the reason for lower performance, however not much improvement was observed. Also, the shrinking of alkaline membrane at higher temperatures might be the result. Figure 4.1 more clearly shows the temperature and current density relation using actual data values.

---

[1] This experimental method is based on the published paper: Kruusenberg, I., Matisen, L., Shah, Q., Kannan, A. M., & Tammeveski, K. (2011). Non-platinum cathode catalysts for alkaline membrane fuel cells. *International Journal of Hydrogen Energy*.nano electrocatlyst

Table 4.1: Effect of operating conditions on AMFC performance

Temperature (°C)	Percentage Current density (%)	Relative Humidity (%)
30	59.5	100
40	73.3	100
45	100	100
50	77.3	100
55	78.1	75-100

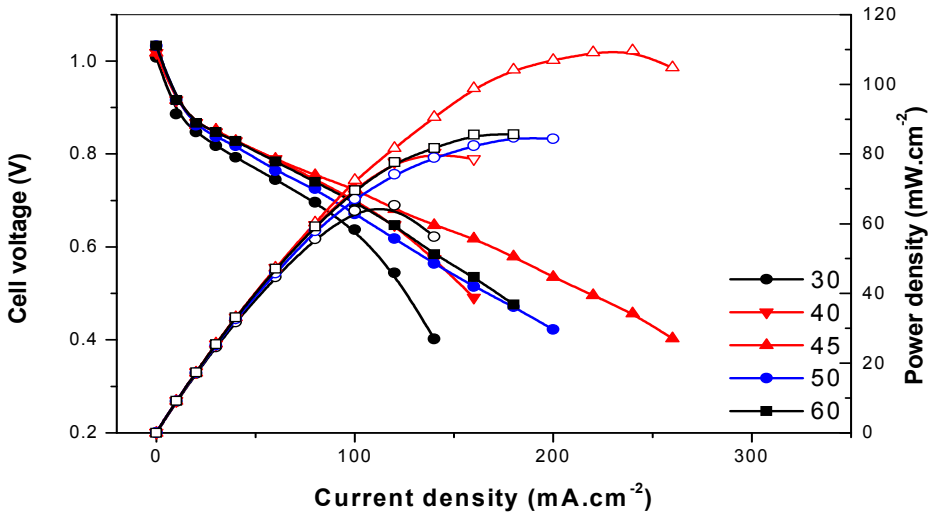

Figure 4.1: Effect of temperature on AMFC performance

4.2. XPS analysis of FePc/MWCNT and CoPc/MWCNT samples

To study the composition of the electrocatalysts surface and to determine the chemical states of the surface species, the X-ray photoelectron spectroscopy (XPS) has been used. Figure 4.2a and 4.2b presents the XPS survey spectra of FePc/MWCNT and CoPc/ MWCNT samples, respectively. Four XPS peaks were observed for both samples, which correspond to emission from C1s, satellite peak of the C1s spectrum, O1s and N1s levels. In addition Fe2p peak has been detected for FePc/MWCNT and Co2p peak for CoPc/MWCNT samples, respectively. The O1s peak is related to the MWCNT material and is caused by various carbon-oxygen functionalities on the surface of CNTs. Detection of different functional groups from the O1s peak is not straightforward because of similar binding energies, but different investigations have shown that quinone and carboxyl groups are present on the surface of carbon nanotubes [60-62]. The XPS core-level spectrum in the N1s region of FePc/MWCNT and CoPc/MWCNT samples shows two peaks. The peak at 399.8 eV could be assigned to N introduced into the graphene layer but the N1s peak at higher binding energy at 400.2 eV corresponds to a new nitrogen species formed likely during the pyrolysis. Similarly to the O1s peak, the exact chemical nature of these surface species is still under debate. Two similar nitrogen peaks to FePc/MWCNT and CoPc/ MWCNT samples have been observed also for CoTPP and ClFeTPP on acetylene black and in this case they were assigned to C-N-H_x and C-N-Me groups evolved from the decomposition of the M-N_4 chelates [63]. From the inset of figure 4.2a

it is possible to observe peaks at 710.5 and 711.5 eV which could correspond to iron oxide and PcFe-OOH groups, respectively. The determination of the exact form of iron oxides on the basis of $Fe2p_{3/2}$ emission is difficult because it is regarded as complex multiplet structure due to the coupling of the core hole to the open valence shell of the Fe atom [64,65]. From the figure 4.2b it is possible to observe the triplet of the peaks of Co2p. The XPS peak at 778.5 eV corresponds to metallic cobalt, peak 780.5 eV which corresponds to Co^{2+} from all CoPc/MWCNT and peak at 781 eV corresponding to pure CoPc [37]. The percentage of different elements in FePc/ MWCNT sample were Fe: 0.3%, N: 4% and O: 4.5% and for CoPc/ MWCNT sample Co: 0.35%, N: 3% and O: 3%. It should be noted that nitrogen or metal catalyst impurities were not detected in the as-received MWCNT samples by XPS.

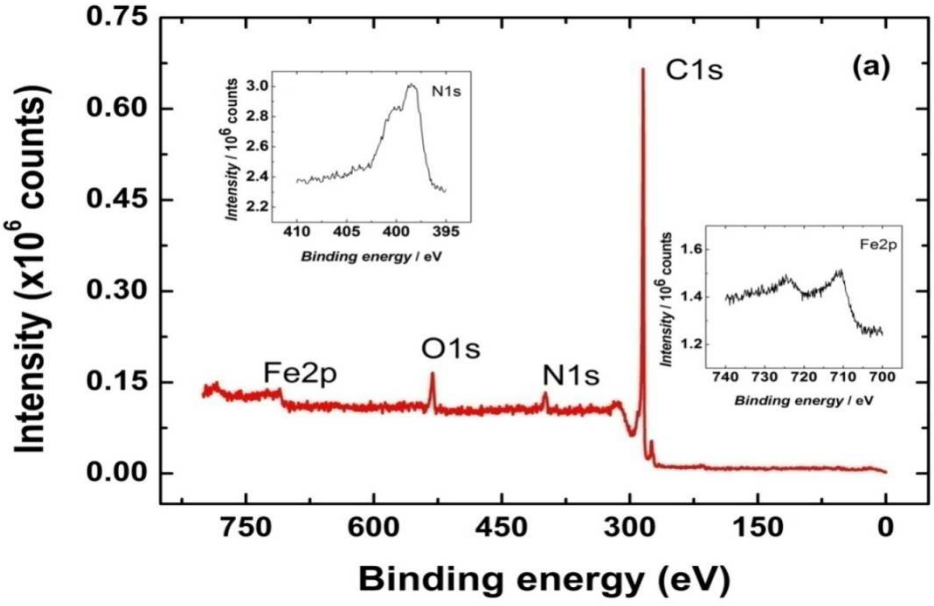

Figure 4.2a: XPS spectra of the FePc/ MWCNT catalyst with inset spectra of N1s and Fe2p

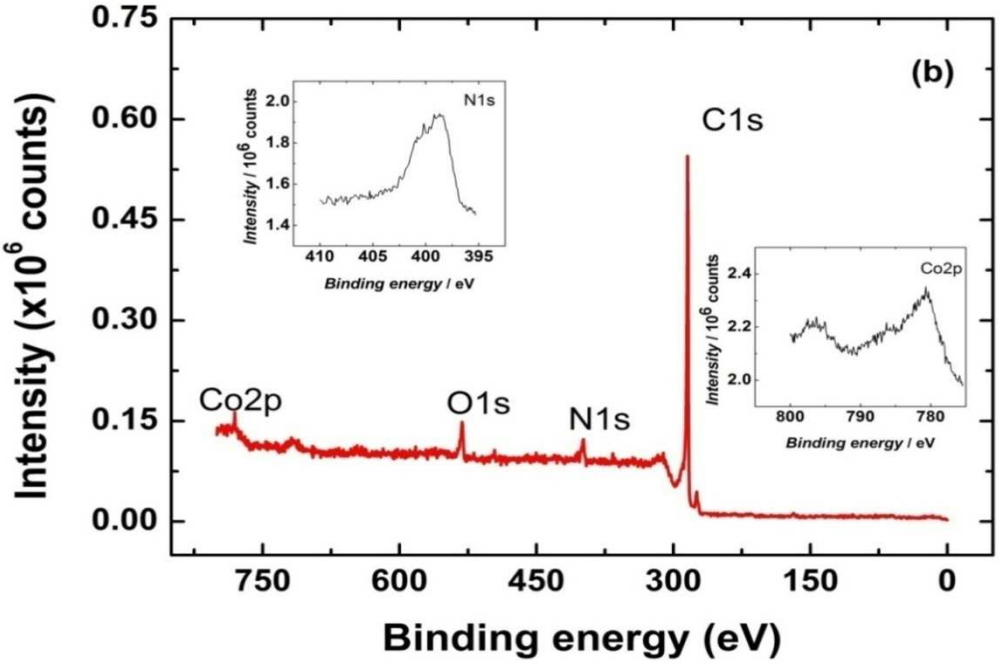

Figure 4.2 b: XPS spectra of the CoPc/ MWCNT catalyst with inset spectra of N1s and Co2p.

4.3. Rotating disk electrode studies of O_2 reduction

The kinetics of the ORR on GC electrodes modified with different catalyst materials was investigated using the RDE method. Figure 4.3a and 4.3 b presents the RDE polarization curves for oxygen reduction on FePc/MWCNT and CoPc/MWCNT modified GC electrodes in O_2 saturated 0.1 M KOH. The RDE results show that the CoPc/MWCNT catalyst material is more active and with higher reduction current density than the FePc/ MWCNT because the onset potential of the oxygen reduction reaction on the CoPc/MWCNT starts at -0.1 V and shifts towards the positive direction as compared to the FePc/ MWCNT

catalyst for which the onset potential is -0.15 V. The limiting current density increases when the rotation rate increases and there is a clear pre-wave present at low over-potentials. The second reduction wave on FePc/MWCNT starts at approximately -0.7 V and on CoPc/MWCNT at approximately -0.6 V.

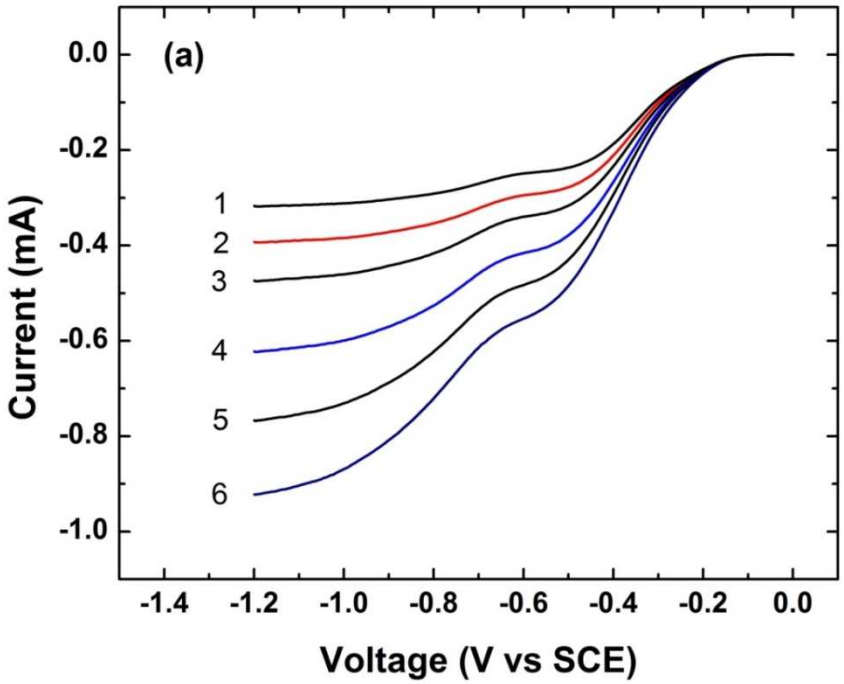

Figure4.3 a: RDE voltammetry curves for oxygen reduction on FePc/MWCNT GC electrodes in O_2 saturated 0.1 M KOH. υ = 10 mV s^{-1}.ω: (1) 360, (2) 610, (3) 960, (4) 1900, (5) 3100 and (6) 4600 rpm.

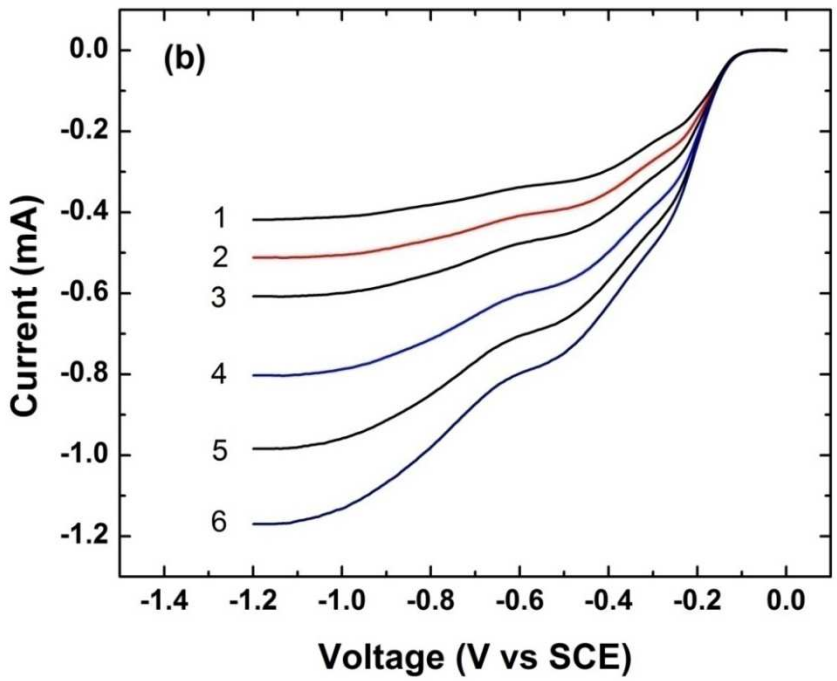

Figure4.3 b: RDE voltammetry curves for oxygen reduction on CoPc/MWCNT modified GC electrodes in O_2 saturated 0.1 M KOH. υ = 10 mV s^{-1}.ω: (1) 360, (2) 610, (3) 960, (4) 1900, (5) 3100 and (6) 4600 rpm.

For the heat-treated FePc/MWCNT and CoPc/MWCNT catalysts a high reduction current density was observed probably because of the generation of electrocatalytically active species which usually form at temperatures from 700 to 950 ^{o}C. Ladouceur et al. have reported that the electrocatalytic activity of CoPc/XC-72, which was annealed at 800 ^{o}C, was twice as high as the activity of the non-pyrolysed CoPc/XC-72 [37]. It has been proposed that the electrocatalytically active sites for ORR could be the central metal ion with N atoms [37]. Even if the metal particles on carbon supports are sometimes reported not to be related to the activity of the catalyst [66] and N not being a part of the

catalytically active site for ORR [67], these two species together form highly active catalyst center for ORR.

The number of electrons transferred per O_2 molecule (n) was calculated from the KouteckyeLevich (KeL) equation [68]

$$\frac{1}{j} = \frac{1}{j_k} + \frac{1}{j_d} = -\frac{1}{nFkc^b_{O_2}} - \frac{1}{0.62nFD^{2/3}_{O_2}\nu^{-1/6}c^b_{O_2}\omega^{1/2}} \quad (4.1)$$

where j is the measured current density, j_k and j_d are the kinetic and diffusion-limited current densities, respectively, k is the electrochemical rate constant for O_2 reduction, D_{O2} is the diffusion coefficient of oxygen (1.9×10^{-5} $cm^2\ s^{-1}$) [69], c^b_{O2} is the concentration of oxygen in the bulk (1.2×10^{-6} mol cm^{-3}) [69], and n is the kinematic viscosity of the solution (0.01 $cm^2\ s^{-1}$) [70].

Figure 4.4a and 4.4b presents the K-L plots obtained from the RDE data on oxygen reduction for FePc/MWCNT (4.4a) and CoPc/ MWCNT (4.4b) at several rotation rates in 0.1 M KOH. The intercepts of the extrapolated K-L lines were close to zero, which shows that the process of O_2 reduction is almost entirely under the diffusion control. The inset of Figure 4.4a and b compares the number of electrons involved in the reduction of O_2 calculated from the K-L equation at various potentials. The inset to Figure 4.4a shows that the value of n for oxygen reduction on the FePc/MWCNT catalyst varies between 2.5 and 3, depending on the potential at high negative potentials. This indicates that the mixed $2e^-$ and $4e^-$ process takes place and the reduction of O_2 produces both HO^-_2 and OH^-.From the inset of Figure 4.4b one can see that for the CoPc/MWCNT material the value of

n is close to 3 at -0.4 V but at more negative potentials the n value gradually increases and approaches almost 4, which indicates that the peroxide formed reduces further to water in this potential range.

A comparison of the RDE data on oxygen reduction recorded on GC electrodes modified with different catalyst materials are presented in Figure 4.5.The commercial catalyst Pt/C 46 wt.% shows a higher reduction current than any other material compared and this is related to the high loading of platinum. At the foot of the polarization curve the commercial catalyst Pt/C 20 wt.% also shows a higher reduction current than phthalocyanines but at more negative potentials the CoPc/MWCNT modified electrode becomes more active and its current rate exceeds the current values of Pt/C 20 wt.% material. FePc/MWCNT also shows the extraordinary ORR performance in alkaline electrolyte but its current is not rising as high as that observed for the CoPc/MWCNT material. The RDE voltammetry curve of unmodified MWCNTs has been also added for comparison purposes. It is clearly evident that the onset potential of O_2 reduction on unmodified MWCNTs is substantially more negative than that of MWCNTs coated with CoPc and FePc. This indicates that the catalyst activity is entirely determined by pyrolysed metallo-phthalocyanines on the surface of MWCNTs. In agreement with previous investigations, the reduction of oxygen on MWCNTs follows a two-electron pathway at low over-potentials and the formed HO_2^- reduces further at more negative potentials [71,72].

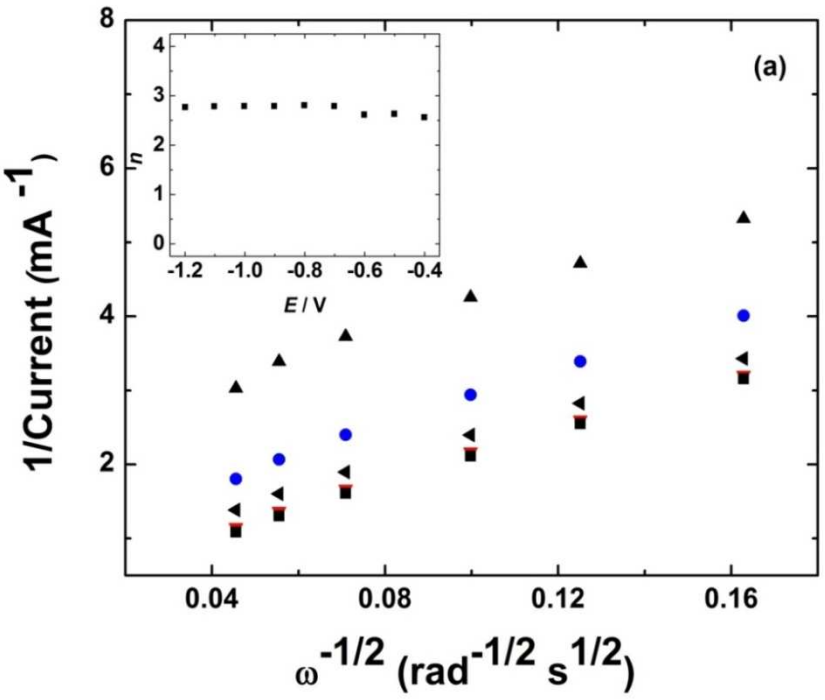

Figure 4.4a: Koutecky-Levich plots for oxygen reduction on FePc/MWCNT electrodes in 0.1 M KOH at various potentials: (●) -0.6, (◀)-1.0, (▼)-0.8, (■) -1.2 and (▲)-0.4 V. The inset shows the potential dependence of n.

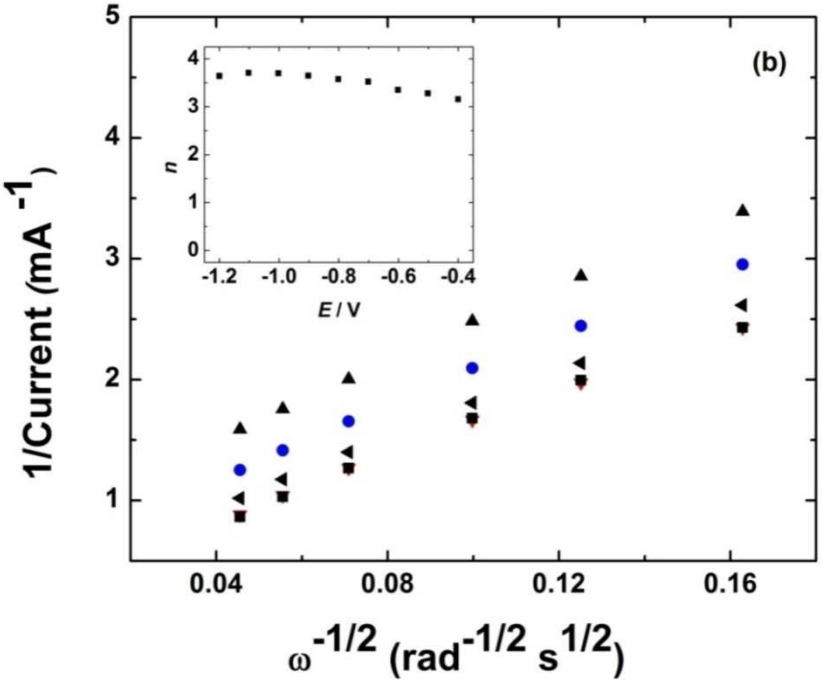

Figure 4.4: Koutecky-Levich plots for oxygen reduction on (a) FePc/MWCNT and (b) CoPc/MWCNT electrodes in 0.1 M KOH at various potentials: (●) -0.6, (◀)-1.0, (▼)-0.8, (■) -1.2 and (▲)-0.4 V. The inset shows the potential dependence of n.

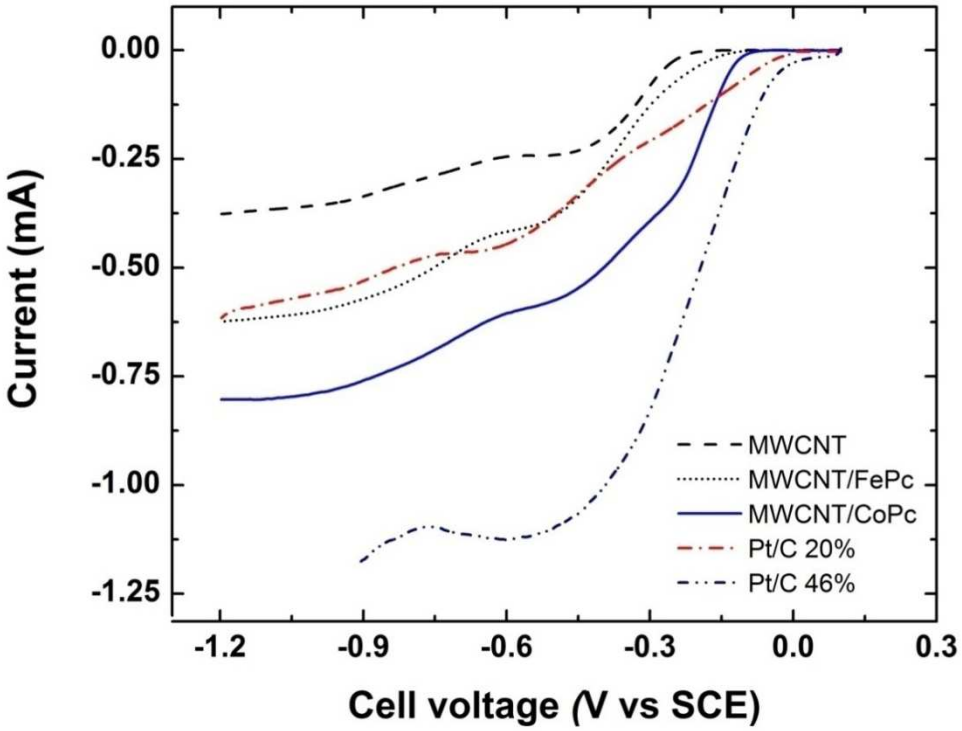

Figure 4.5: RDE voltammetry curves for oxygen reduction on different catalyst material modified GC electrodes in O_2 saturated 0.1 M KOH. υ = 10 mV s^{-1}. ω: 1900 rpm.

4.4. Fuel cell performance of FePc/MWCNT and CoPc/MWCNT catalysts

All the fuel cell testing results presented in this section were carried out at ~45 $^{\circ}$C in a single cell fuel cell and with 100% relative humidity. Figure 4.6 compares the fuel cell performance of MEAs with FePc/ MWCNT and CoPc/MWCNT cathode electrocatalysts using humidified H_2 and O_2 gases. In order to compare the performance of these non-noble metal catalysts, two commercial Pt/C catalysts (E-TEK and Tanaka) were also evaluated and the performance compared at identical operating conditions. As can be seen from the figure, Tanaka Pt/C catalyst showed the highest performance (~120 mW cm^{-2}).

CoPc/MWCNT performed almost (power density ~100 mW cm^{-2}) similar to that of the E-TEK catalyst based MEAs. However, the FePc/MWCNTs based MEA showed about 60 $mW.cm^{-2}$ only, under similar conditions. MEAs with bare MWCNT based cathodes were also evaluated to see whether there was any ORR activity. Evidently, MWCNTs showed poor performance with lower OCV also. The fuel cell performance of the MEAs became fluctuating above $50^{o}C$, probably due to water balance issues in the cell and shrinking of OH membrane. However, the reported power density with Tokuyma membrane was about 180 mW cm^{-2} using Co-Fe/C catalysts by Li et al. [30]. Recent literature on the AFC using Pt catalyst ink with aminated tetramethyl polysulfone membrane showed much poorer performance even with 2 mgPt cm^{-2} under high operating pressure [73]. Work is in progress to optimize the operating conditions to improve the performance at elevated temperatures. Further work is also in progress to evaluate Tokuyama membrane #901 with 10 mm thickness.

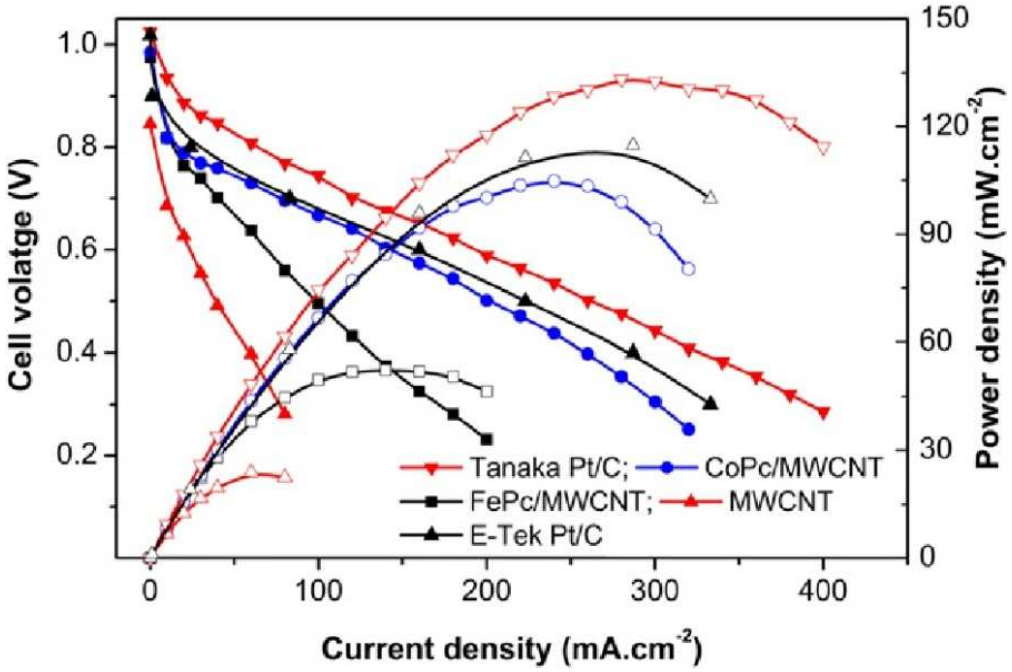

Figure 4.6: Fuel cell performance of MEAs with Co and Fe phthalocyanine modified MWCNTs along with E-TEK and Tanaka Pt/C catalysts based cathodes using Tokuyama's A201 series anion exchange membrane.

4.4.1. Comparison of CoPc in AMFC with Air and O_2

Figure 4.7 shows the performance of H_2/Air and H_2/O_2 based AMFC, with CoPc as cathode catalysts. When operating with air, current density reduces ~ 50-60% compared to H_2/O_2. This is loss in performance is in accordance with the fuel cell that uses Pt/C and operates on air. Therefore, as solid polymer alkaline fuel cells, they have potential to run on air as well unlike liquid electrolyte alkaline fuel cells that suffer from carbon dioxide poisoning.

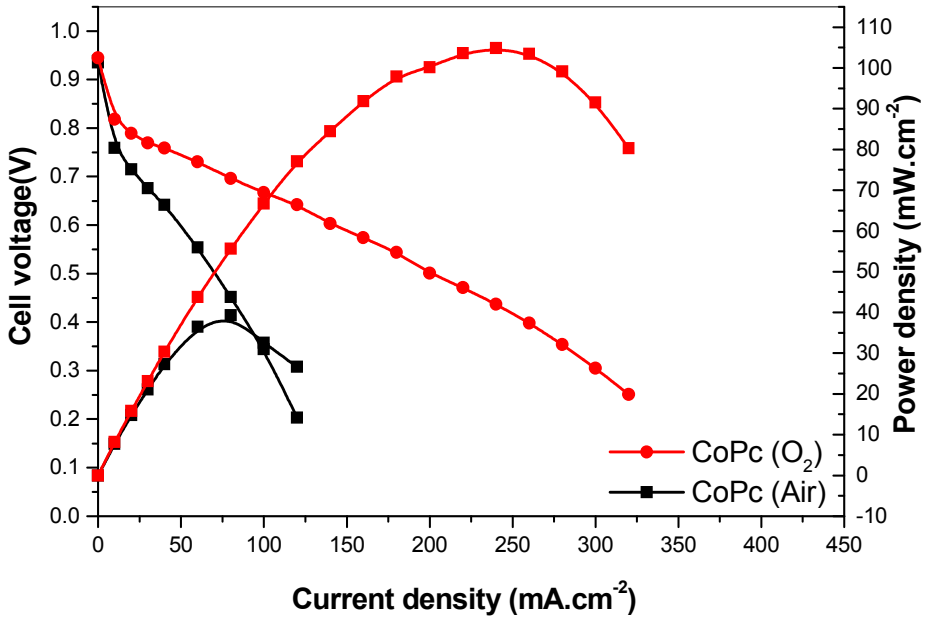

Figure 4.7: Performance comparison of CoPc in H_2/O_2 and H_2/Air H_2/Air

4.4.2. Performance comparison between AMFC and PEMFC

Figure 4.8 shows the performance of non-noble electrocatalyst CoPc in PEMFC (Nafion membrane) and AMFC (OH^- membrane). Following points discuss the main differences in the parameters of the polarization curve of two fuel cells:

1. CoPc performance in proton exchange membrane fuel cell
    a. There is high activation loss in PEMFC due to poor activity of the Cobalt phthalocyanine catalyst in the acidic medium [39].
    b. PEMFC has lower IR loss because of higher conductivity of the Nafion membrane which is 0.10 $S.cm^{-2}$.

2. CoPc performance in alkaline membrane fuel cell

    a. There is lower activation loss in AMFC which shows that the CoPc catalyst is more active and efficient in the alkaline medium.

    b. Due to lower Ionic conductance of 11 mS .cm^{-2} of OH membrane (# A201), IR loss is higher in AMFC.

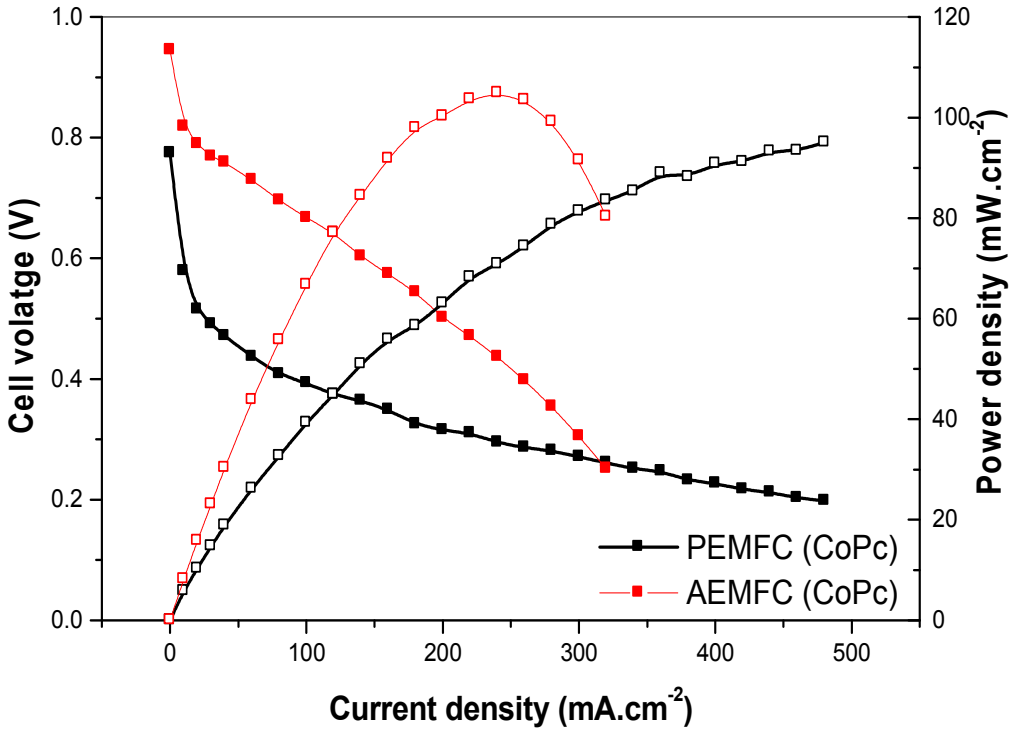

Figure 4.8: Performance comparison of CoPc cathode catalyst in PEMFC and AMFC with H_2/O_2

4.5. Nitrogen doped MWCNT

4.5.1. Nitrogen doped MWCNT (post-doping) performance in AMFC

The post-treated nitrogen doped MWCNT were characterized through fuel cell testing, by comparing it with pristine MWCNT and FePc/MWCNT cathode catalysts in AMFC. It can be seen from Figure 4.9 that N/MWCNT cathode catalyst gave power density of ~ 40 $mW.cm^{-2}$ and performed better than pristine MWCNT. As a non-noble electrocatalyst, nitrogen doped MWCNT could be applied to the design and development of various metal free efficient ORR catalysts, even to new materials for applications beyond fuel cells [74].

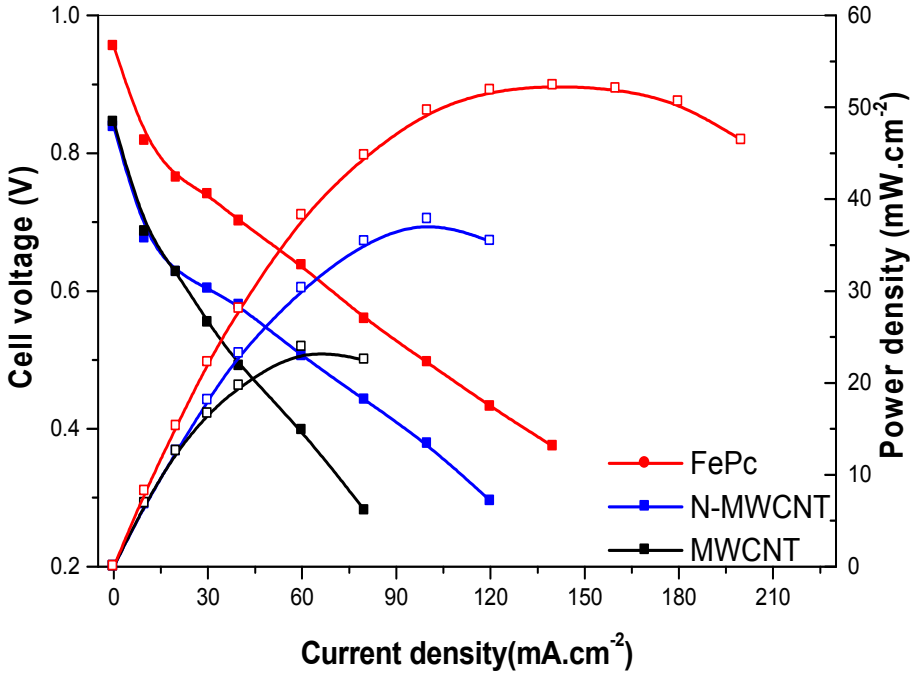

Figure 4.9: Fuel cell performance comparison between FePc/MWCNT, N-MWCNT and pristine MWCNT

4.5.2. Raman Spectroscopy

The degree of structural deformations in the MWCNT and N doped MWCNT samples is evaluated using Raman spectroscopy. Two distinct bands D and G can be observed from Figure 4.10. The D band, at approximately 1345 cm^{-1} for the samples due to the disorder induced, which is generally attributable to structural defects and other disordered structures on the graphitic-like plane [56]. The G band, at approximately 1570 cm^{-1}, is commonly observed for all graphitic-like structures and can be attributed to the E_{2g} vibrational mode present in the sp^2 bonded graphitic carbons.

The intensity ratio of D band to G band, namely the I_D /I_G ratio is calculated as it is helpful in finding the amount of structural defects. It is also known that I_D /I_G ratio increases linearly with nitrogen doping of multi-walled carbon nanotubes [75,76]. N doped MWCNT was found to have an I_D /I_G ratio of 1.12, and value of 0.9 was observed for MWCNT. It can be seen that N doped MWCNT has larger I_D /I_G ratio, which is a result of the structural defects and edge plane exposure caused by nitrogen atom incorporation [56].Various studies concluded that higher nitrogen content and more defects result in higher ORR performance. Moreover, studies suggests that in nitrogen doped CNTs, the pyridinic form of nitrogen is the main contributor in the disorder-induced in CNT walls [56]

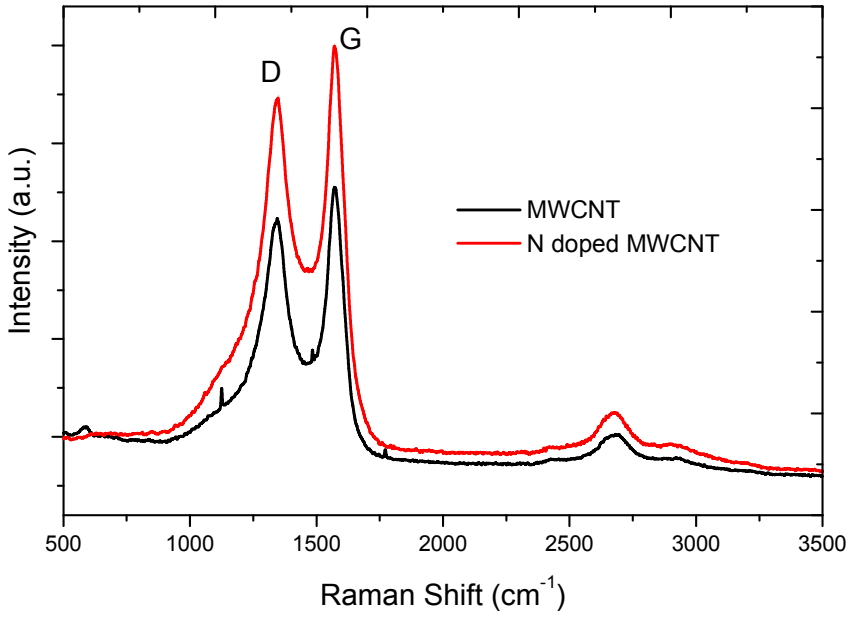

Figure 4.10: Raman spectra for nitrogen doped MWCNT and pristine MWCNT

Three different forms of nitrogen have been identified in N doped carbon nanotubes [51-55]:

1. Graphitic nitrogen (carbon atom in graphitic network is substituted for nitrogen atom);
2. Pyridinic nitrogen (nitrogen atom is positioned at the edge of an atomic vacancy); and
3. Molecular nitrogen trapped by CNT.

It is reported that graphitic and pyridinic nitrogen atoms are directly incorporated in the nanotube walls and could be responsible for the increase of structural imperfection of CNTs with doping.

4.5.3. Rutherford Backscattering Spectroscopy (RBS)

Figure 4.11 compares Rutherford backscattering spectra for the MWCNT and N-MWCNT samples. It clearly shows saturation of the nitrogen peak concentration for N-MWCNT sample which is absent for MWCNT sample, which suggests the occurrence of nitrogen on the surface nanotubes. A quantitative analysis of the RBS data by a computer simulation shows that the peak concentration of nitrogen in N-MWCNT is ~3 at. %. Table 4.2 shows atomic percentage of nitrogen and other elements present in N/MWCNT.

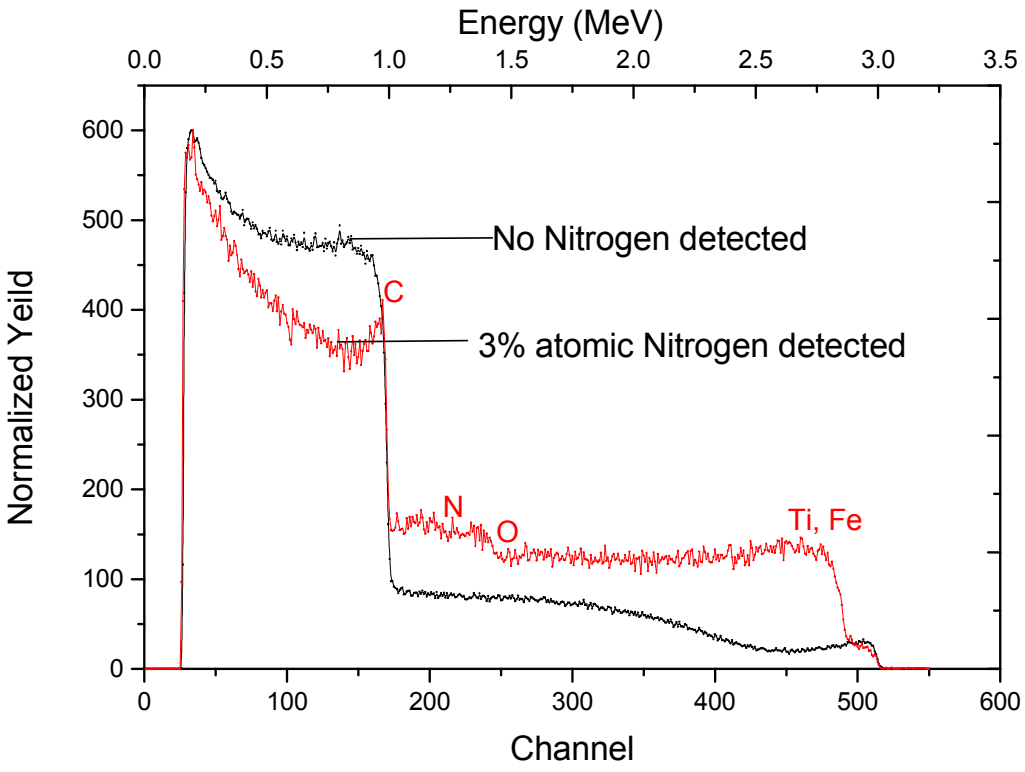

Figure 4.11: RBS spectra for nitrogen doped MWCNT and pristine MWCNT sample

Table 4.2: At. % of various materials constituting N-MWCNT

Elements	Atomic Percentage (%)
Fe	2
Ti	6
O	2
C	87
N	3

4.6. Economic analysis

Economic analysis was done at the end to understand the feasibility of the non-noble catalysts compared to Pt. Table 4.3 presents the economic analysis for different types of AMFC cathode catalysts. Figure 4.12 and 4.13 shows performance to cost ratio, which is found to be highest in CoPc with 36 followed by FePc, N/MWCT and then Pt.

Table 4.3: Economic analysis of various cathode catalysts for AMFC

Sample #	Catalyst	Cost ($)	Cost/(gm or ml) ($)	Electrode cost ($)	Power density (mW. cm^{-2})	Performance / Cost Ratio ($mW.cm^{-2}/\$$)
1	Pt/C (46%)	60/gm	27.6	16.56	120	7.24
2	CoPc (97%)	23/5gm	4.6	2.76	100	36.23
3	FePc (97%)	25/5gm	5	3	60	20
4	NH_4OH (50%)	$45/500 ml	5.6	3.3	40	12

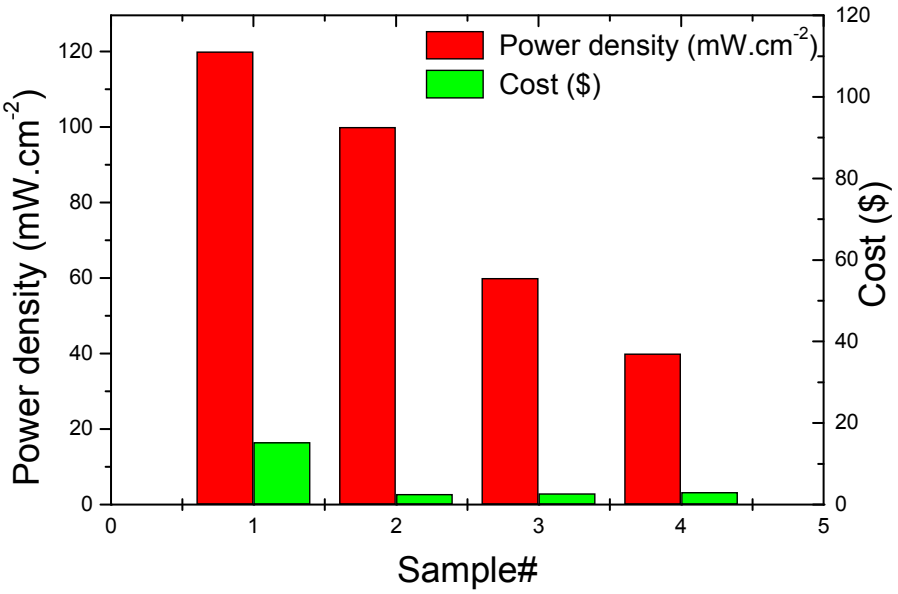

Figure4.12: Individual power density and cost plots for catalyst samples

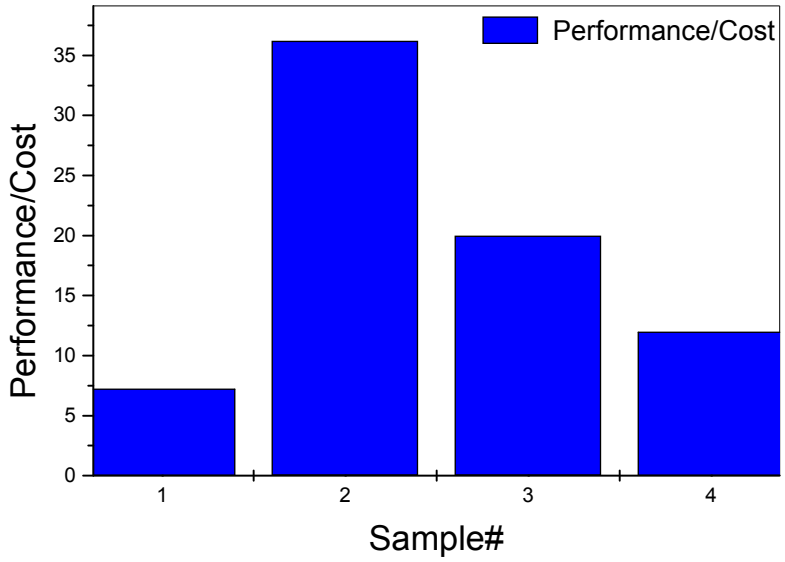

Figure4.13: Performance to cost ratio of the catalyst samples

Chapter 5

CONCLUSION

Non-noble metal electrocatalysts namely Co and Fe phthalocyanines were supported on multi-walled carbon nanotubes with 50% loading through a simple thermal method. The surface composition of MWCNT supported Co and Fe phthalocyanines were examined by XPS. The XPS results showed the decomposition of the phthalocyanine ring because of the pyrolysis and the formation of the different electrocatalytically active metallic and nitrogen surface groups. These non-noble catalysts were also evaluated towards the ORR kinetics by RDE method in 0.1 M KOH and it was found that Co phthalocyanine based electrodes performed well compared to Fe phthalocyanine. Membrane electrode assemblies were fabricated using catalyst coated Tokuyama[3] membrane (# A201) and compared with E-TEK and Tanaka commercial Pt/C catalysts. The fuel cell performance of the MEAs with Co phthalocyanine/MWCNT cathode was found to be only slightly inferior to Tanaka Pt/C cathode catalysts but similar to that with E-TEK catalysts using H_2 and O_2 gases.

Work on synthesize of N doped MWCNT was performed using post-doped and In-Situ methods; NH_4OH and pyridine were employed respectively as nitrogen sources. Raman spectra and RBS illustrated the presence of doped nitrogen on the carbon surface. Performance evaluation using fuel cell testing was done. Furthermore, economic analysis was done in which CoPc/MWCNT cathode electrode showed highest performance to cost ratio in AMFC.

It can be recommended for future work to explore more efficient and low cost catalyst materials with stable N-MWCNT GDL to achieve higher AMFC performance. Also, work on anode fuels using the formate salts can be carried out in future studies.

REFERENCES

[1] Alkaline fuel cells applications , Karl Kordesch,Viktor Hacker, Josef Gsellmann, Martin Cifrain b , Gottfried Faleschini a , Peter Enzinger a , Robert Fankhauser a , Markus Ortner a , Michael Muhr a , Robert R. Aronson c

[2] J. Larminie, A. Dicks, "Fuel Cell Systems Explained," England: Wiley, 2003

[3] S. Lasher, J. Sinha, Y. Yang, S. Sriramulu, "Direct Hydrogen PEMFC Manufacturing Cost Estimation for Automotive Applications," August 2009, Available: http://www1.eere.energy.gov/hydrogenandfuelcells/fc_publications.html

[4] Fuel cells basic . (n.d.). In Fuel cells. Retrieved March 27, 2012 from [http://americanhistory.si.edu/fuelcells/basics.htm]

[5] If you took all of the gold in the world and put it in one place how much would there be?. In How stuff works?. Retrieved March 27, 2012 from http://money.howstuffworks.com/question213.htm

[6] Gulzow, E. (2004, July). Alkaline fuel cells. Fuel cells 2004.

[7] Merle, G., Wessling, M., & Nijmeijer, K. (2011, April 30). Review Anion exchange membranes for alkaline fuel cells: A review.Journal of Membrane Science, 1-35.

[8] J. Zhang. PEM Fuel Cell Electrocatalysts and Catalyst Layers: Fundamentals and Applications. Springer-Verlag London Ltd, Gulldford, Surrey,U.K, 2008

[9] Variation of Compression of Seals in PEM Fuel Cells (Experimental and Applied Mechanics) . (n.d.). Retrieved 27, 2012 from http://what-when-how.com/experimental-and-applied-mechanics/variation-of-compression-of-seals-in-pem-fuel-cells-experimental-and-applied-mechanics/

[10] Modeling of frost heave during freezing in polymer electrolyte fuel cells. Doctoral Thesis / Dissertation, 2007, 210 Pages. Retrieved 2012 from http://www.grin.com/en/doc/231060/modeling-of-frost-heave-during-freezing-in-polymer-electrolyte-fuel-cells

[11] Gewirth A, Thorum M. Electroreduction of dixoygen for fuel cell applications: materials and challenges. Inorg Chem 2010; 49:3557e66.

[12] Lin JF, Kamavaram V, Kannan AM. Synthesis and characterization of CNT supported platinum nanocatalyst for PEMFCs. J Power Sources 2010;195:466e70.

[13] Wang C, Waje M, Wang X, Tang JM, Haddon RC, Yan YS. Proton exchange fuel cell with carbon nanotube based electrode. Nano Lett 2004;4:345e8.

[14] Kannan AM, Xiong L, Manthiram A. Pt-M (M ¼ Fe, Co, Ni and Cu) electrocatalysts synthesized by an aqueous route for proton exchange membrane fuel cells. Electrochem Commun 2002;4:898e903.

[15] Mougenot M, Caillard A, Brault P, Baranton S, Coutanceau C. High performance plasma sputtered PdPt fuel cell electrodes with ultra low loading. Int J Hydrogen Energy 2011;36: 8429e34.

[16] Martin S, Garcia-Ybarra PL, Castillo JL. High platinum utilization in ultra-low Pt loaded PEM fuel cell cathodes prepared by electrospraying. Int J Hydrogen Energy 2010;35: 10446e51.

[17] Ahluwalia RK, Wang X, Kwon J, Rousseau A, Kalinoski J, James B, et al. Performance and cost of automotive fuel cell systems with ultra-low platinum loadings. J Power Sources 2011;196:4619e30.

[18] Billy E, Maillard F, Morin A, Guetaz L, Emieux F, Thurier C, et al. Impact of ultra-low Pt loadings on the performance of anode/cathode in a proton-exchange membrane fuel cell. J Power Sources 2010;195:2737e46.

[19] Saha MS, Gulla´ AF, Allen RJ, Mukerjee S. High performance polymer electrolyte fuel cells with ultra-low Pt loading electrodes prepared by dual ion-beam assisted deposition. Electrochim Acta 2006;51:4680e92.

[20] Bashyam R, Zelenay P. A class of non-precious metal composite catalysts for fuel cells. Nature 2006;443:63e6.

[21] Lefe`vre M, Proietti E, Jaouen F, Dodelet JP. Iron-based catalysts with improved oxygen reduction activity in polymer electrolyte fuel cells. Science 2009;324:71e4.

[22] Wu G, More KL, Johnston CM, Zelenay P. High-performance electrocatalysts for oxygen reduction derived from polyaniline, iron, and cobalt. Science 2011;332:443e7.

[23] Jasinski R. A new fuel cell cathode catalyst. Nature 1964;201: 1212e3.

[24] Yuan Y, Ahmed J, Kim S. Polyaniline/carbon black composite-supported iron phthalocyanine as an oxygen reduction catalyst for microbial fuel cells. J Power Sources 2011;196:1103e6.

[25] Baranton S, Coutanceau C, Roux C, Hahn F, Le´ger J-M. Oxygen reduction reaction in acid medium at iron phthalocyanine dispersed on high surface area carbon substrate: tolerance to methanol, stability and kinetics. J Electroanal Chem 2005;577:223e34.

[26] Kavelage H, Mecklenburg A, Kunz U, Hoffmann U. Electrochemical reduction of oxygen at pyrolyzed iron and cobalt N4-chelates on carbon black supports. Chem Eng Technol 2000;23:803e7.

[27] Claude E, Addou T, Latour J-M, Aldebert P. A new method for electrochemical screening based on the rotating ring disc electrode and its application to oxygen reduction catalysts. J Appl Electrochem 1997;28:57e64.

[28] Lalande G, Faubert G, Coˆte´ R, Guay D, Dodelet JP, Weng LT, et al. Catalytic activity and stability of heat-treated iron phthalocyanines for the electroreduction of oxygen in polymer electrolyte fuel cells. J Power Sources 1996;61: 227e37.

[29] Bambagioni V, Bianchini C, Filippi J, Lavacchi A, Oberhauser W, Marchionni A, et al. Single-site and nanosized FeeCo electrocatalysts for oxygen reduction: synthesis, characterization and catalytic performance. J Power Sources 2011;196:2519e29.

[30] Li X, Popov BN, Kawahara T, Yanagi H. Non-precious metal catalysts synthesized from precursors of carbon, nitrogen, and transition metal for oxygen reduction in alkaline fuel cells. J Power Sources 2011;196:1717e22.

[31] Mamuru SA, Ozoemena KI. Heterogeneous electron transfer and oxygen reduction reaction at nanostructured iron(II) phthalocyanine and its MWCNTs nanocomposites. Electroanalysis 2010;22:985e94.

[32] Yuan Y, Zhao B, Jeon Y, Zhong S, Zhou S, Kim S. Iron phthalocyanine supported on amino-functionalized multi-walled carbon nanotube as an alternative cathodic oxygen catalyst in microbial fuel cells. Bioresour Technol 2011;102: 5849e54.

[33] V. Kamavaram, V. Veedu and A.M. Kannan. Synthesis and characterization of platinum nanoparticles on in situ grown carbon nanotubes based carbon paper for proton exchange membrane fuel cell cathode. J. Power Sources, 188 (2009): 51-56

[34] Zagal JH, Griveau S, Ozoemena KI, Nyokong T, Bedioui F. Carbon nanotubes, phthalocyanines and porphyrins: attractive hybrid materials for electrocatalysis and electroanalysis. J Nanosci Nanotechnol 2009;9:2201e14.

[35] Xu Z, Li H, Cao G, Zhang Q, Li K, Zhao X. Electrochemical performance of carbon nanotube-supported cobalt phthalocyanine and its nitrogen-rich derivatives for oxygen reduction. J Mol Catal A Chem 2011;335:89e96.

[36] Li H, Xu Z, Li K, Hou X, Cao G, Zhang Q, et al. Modification of multi-walled carbon nanotubes with cobalt phthalocyanine: effects of the templates on the assemblies. J Mater Chem 2011;21:1181e6.

[37] Ladouceur M, Lalande G, Guay D, Dodelet JP, Dignard-Bailey L, Trudeau ML, et al. Pyrolyzed cobalt phthalocyanine as electrocatalyst for oxygen reduction. J Electrochem Soc 1993;140:1974e81.

[38] Lu Y, Reddy RG. Electrocatalytic properties of carbon supported cobalt phthalocyanine-platinum for methanol electro-oxidation. Int J Hydrogen Energy 2008;33:3930e7.

[39] Zhang, L., Zhang, J., Wilkinson, D. P., & Wang, H. (2005, July). Progress in preparation of non-noble electrocatalysts for PEM fuel cell reactions. Journal of Power Sources.

[40] Yu EH, Cheng S, Logan BE, Scott K. Electrochemical reduction of oxygen with iron phthalocyanine in neutral media. J Appl Electrochem 2009;39:705e11.

[41] Morozan A, Camidelli S, Filoramo A, Jousselme B, Palacin S. Catalytic activity of cobalt and iron phthalocyanines or porphyrins supported on different carbon nanotubes towards oxygen reduction reaction. Carbon 2011;49:4839e47.

[42] Merle G, Wessling M, Nijmeijer K. Anion exchange membranes for alkaline fuel cells: a review. J Membrane Sci 2011;377:1e35.

[43] Surya Prakash GK, Krause FC, Viva FA, Narayanan SR, Olah GA.

Study of operating conditions and cell design on the performance of alkaline anion exchange membrane based direct methanol fuel cells. J Power Sources 2011;196:7967e72.

[44] Lee KM, Wycisk R, Litt M, Pintauro PN. Alkaline fuel cell membranes from xylylene block ionenes. J Membrane Sci 2011;383:254e61.

[45] Couture G, Alaaeddine A, Boschet F, Ameduri B. Polymeric materials as anion-exchange membranes for alkaline fuel cells. Prog Polymer Sci 2011;36:1521e57.

[46] Nikolic VM, Zugic DL, Maksic AD, Saponjic DP, Kaninski MPM. Performance comparison of modified poly(vinyl alcohol) based membranes in alkaline fuel cells. Int J Hydrogen Energy 2011;36:11004e10.

[47] Ong AL, Saad S, Lan R, Goodfellow RJ, Tao S. Anionic membrane and ionomer based on poly(2,6-dimethyl-1,4-phenylene oxide) for alkaline membrane fuel cells. J Power Sources 2011;196:8272e9.

[48] Nagaiah, T. C., Kundu, S., Bron, M., Muhler, M., & Schuhmann, W. (2009, December). Nitrogen-doped carbon nanotubes as a cathode catalyst for the oxygen reduction reaction in alkaline medium. Electrochemistry Communications.

[49] Subramanian, N. P., Li, X., & Nallathambi, V. (2008, November). Nitrogen-modified carbon-based catalysts for oxygen reduction reaction in polymer electrolyte membrane fuel cells. Journal of Power Sources.

[50] Sidik, R. A., & Anderson, A. B. (2006). O 2 Reduction on Graphite and Nitrogen-Doped Graphite: Experiment and Theory. J. Phys. Chem..

[51] Ayala, P., Arenal, R., & Rummeli, M. (2010). The doping of carbon nanotubes with nitrogen and their potential applications. CA RBON.

[52] Shao, Y., Sui, J., Yin, G., & Gao, Y. (2008). Nitrogen-doped carbon nanostructures and their composites as catalytic materials for proton exchange membrane fuel cell. Applied Catalysis B: Environmental, 89-99.

[53] C.P. Ewels, M. Glerup, J. Nanosci. Nanotechnol. 5 (2005) 1345.

[54] Jaouen, F., Lefevre, M., Dodelet, J., & Cai, M. (2006). Heat-Treated Fe/N/C Catalysts for O 2 Electroreduction: Are Active Sites Hosted in Micropores? J. Phys. Chem..

[55] Liu J, Webster S, Carroll DL. Temperature and flow rate of NH3 effects on nitrogen content and doping environments of carbon nanotubes grown by injection CVD method. J Phys Chem B 2005;109(33):15769–74.

[56] Geng, D., Yang, S., & Zhang, Y. (2011, June). Nitrogen doping effects on the structure of graphene. Applied Surface Science.

[57] Bartrom, A. M., & Haan, J. L. The Direct Formate Fuel Cell with an Alkaline Anion Exchange Membrane. Journal of Power Sources.

[58] Lan, R., & Tao, S. Preparation of nano-sized nickel as anode catalyst for direct urea and urine fuel cells.

[59] Wang X, Li M, Golding BT, Sadeghi M, Cao Y, Yu EH, et al. A polytetrafluoroethylene-quaternary 1,4-diazabicyclo-[2.2.2]-octane polysulfone composite membrane for alkaline anion exchange membrane fuel cells. Int J Hydrogen Energy 2011; 36:10022e6.

[60] Kannan AM, Sadananda S, Parker D, Munukutla L, Wertz J, Thommes M. Wire rod coating process of gas diffusion layers fabrication for proton exchange membrane fuel cells. J Power Sources 2008;178:231e7.

[61] Masheter AT, Xiao L, Wildgoose GG, Crossley A, Jones JH, Compton RG. Voltammetric and X-ray photoelectron spectroscopic fingerprinting of carboxylic acid groups on the surface of carbon nanotubes via derivatisation with arylnitro labels. J Mater Chem 2007;17:3515e24.

[62] Wildgoose GG, Abiman P, Compton RG. Characterising chemical functionality on carbon surfaces. J Mater Chem 2009;19:4875e86.

[63] Widelo¨v A, Larson R. ESCA and electrochemical studies on pyrolysed iron and cobalt tetraphenylporphyrins. Electrochim Acta 1992;37:187e97.

[64] Ouedraogo GV, Benlian D, Porte L. X-ray photoelectron spectroscopy of phthalocyanine compounds. J Chem Phys 1980;73:642e7.

[65] Schmitt F, Sauther J, Lach S, Ziegler C. Characterization of the interface interaction of cobalt on top of copper-and iron-phthalocyanine. Anal Bioanal Chem 2011;400: 665e71.

[66] Wiesener K. N4-chelates as electrocatalyst for cathodic oxygen reduction. Electrochim Acta 1986;3:1073e8.

[67] Alves MCM, Dodelet JP, Guay D, Ladouceur M, Tourillon G. Origin of the electrocatalytic properties for O_2 reduction of some heat-treated polyacrylonitrile and phthalocyanine cobalt compounds adsorbed on carbon black as probed by electrochemistry and X-ray absorption spectroscopy. J Phys Chem 1992;96:10898e905.

[68] Bard AJ, Faulkner LR. In: Electrochemical methods. 2nd ed. New York: Wiley; 2001.

[69] Davis RE, Horvath GL, Tobias CW. The solubility and diffusion coefficient of oxygen in potassium hydroxide solutions. Electrochim Acta 1967;12:287e97.

[70] Lide DR. In: CRC handbook of chemistry and physics. 82nd ed. Boca Raton: CRC Press; 2001.

[71] Jurmann G, Tammeveski K. Electroreduction of oxygen on multi-walled carbon nanotubes modified highly oriented pyrolytic graphite electrodes in alkaline solution. J Electroanal Chem 2006;597:119e26.

[72] Kruusenberg I, Alexeyeva N, Tammeveski K. The pH-dependence of oxygen reduction on multi-walled carbon nanotube modified glassy carbon electrodes. Carbon 2009;47: 651e8.

[73] Switzer EE, Olson TS, Datye AK, Atanassov P, Hibbs MR, Fujimoto C, et al. Novel KOH-free anion-exchange membrane fuel cell: Performance comparison of alternative anion-exchange ionomers in catalyst ink. Electrochim Acta 2010;55:3404e8.

[74] Nitrogen-doped carbon nanotube catalyst systems for low-cost fuel cells. (n.d.). In Nanotechnology for development. Retrieved March 29, 2012 from http://www.nanowerk.com/spotlight/spotid=9177.php

[75] Venkateswara Ra, C., Cabrera, C. R., & Ishikawa, Y. (2010, August). In Search of the Active Site in Nitrogen-Doped Carbon Nanotube Electrodes for the Oxygen Reduction Reaction. J. Phys. Chem..

[76] Bulusheva, L. G., Okotrub, A. V., & Kinloch, I. A. (2008). Effect of nitrogen doping on Raman spectra of multi-walled carbon nanotubes.